Journal of Materials Chemistry A

REVIEW

View Article Online
View Journal | View Issue

Check for updates

Cite this: J. Mater. Chem. A, 2019, 7, 24738

Mixed-matrix membranes for CO_2 separation: role of the third component†

Xiangyu Guo, [ab] Zhihua Qiao,[ab] Dahuan Liu*[cd] and Chongli Zhong *[abcd]

Received 16th August 2019
Accepted 3rd October 2019

DOI: 10.1039/c9ta09012f

rsc.li/materials-a

Mixed-matrix membranes (MMMs) have exhibited excellent performances for CO_2 separation, but it is still an ongoing challenge to enhance the separation performance through optimization of their structures. Recent studies demonstrated that the introduction of a tertiary component may play a positive role in improving the separation performance of two-component MMMs (polymer matrix and filler), showing great promise for addressing this challenge. Herein, recent advances in different types of tertiary components adopted in MMMs for CO_2 separation are reviewed, including small molecules, macromolecules, and porous materials, and a concise conclusion and outlook are outlined toward ternary MMM fabrication.

Published on 04 October 2019. Downloaded by Yunnan University on 8/23/2025 5:29:10 PM.

1 Introduction

Growing concern about global warming and desire for clean energy have increasingly highlighted the importance of pre- and post-combustion CO_2 capture and separation.[1–3] Current technologies such as pressure swing adsorption (PSA), cryogenic separation and chemical scrubbing are still suffering from their equipment investment, energy consumption, or/and environmental impact issues. In contrast, membrane-based separation has gradually gained recognition for being a promising candidate for economical, efficient, and environmentally friendly CO_2 capture and separation.[4–8] During the development of membrane-based separation, various strategies have been proposed to address the trade-off issue between permeability and selectivity commonly existing in polymer membranes, where the preparation of mixed-matrix membranes (MMMs) is considered as the most promising way.[9–12]

MMMs are a class of membranes prepared by uniformly distributing fillers in a polymer matrix, as shown in Fig. 1.[13] The morphology and separation performance of MMMs are affected simultaneously by the properties of filler and polymer materials. This kind of membrane is expected to combine the advantages of polymers in mechanical properties, processability and cost, with the strength of fillers in terms of permeability and selectivity, thus breaking the regulative trade-off between permeability and selectivity of pure polymer membranes.[14–17]

[a]State Key Laboratory of Separation Membranes and Membrane Processes, Tianjin Polytechnic University, Tianjin 300387, China. E-mail: zhongchongli@tjpu.edu.cn
[b]School of Chemistry and Chemical Engineering, Tianjin Polytechnic University, Tianjin 300387, China
[c]College of Chemical Engineering, Beijing University of Chemical Technology, Beijing 100029, China. E-mail: liudh@mail.buct.edu.cn
[d]Beijing Advanced Innovation Center for Soft Matter Science and Engineering, Beijing 100029, China

† Electronic supplementary information (ESI) available. See DOI: 10.1039/c9ta09012f

Xiangyu Guo received his PhD degree in chemical engineering from the Beijing University of Chemical Technology in 2017 and continued his research as a postdoc in the group of Professor Chongli Zhong at Tianjin Polytechnic University. His research mainly focuses on the design and preparation of novel mixed-matrix membranes with optimal structure and separation performance based on advanced nanoporous materials.

Zhihua Qiao received his PhD degree in chemical engineering at Tianjin University in 2015 and continued his research as a postdoc at Tianjin University, until he joined the group of Professor Chongli Zhong at Tianjin Polytechnic University in 2017. His current research mainly focuses on large-area ultra-thin membrane fabrication.

This journal is © The Royal Society of Chemistry 2019

Published on 04 October 2019. Downloaded by Yunnan University on 8/23/2025 5:29:10 PM.

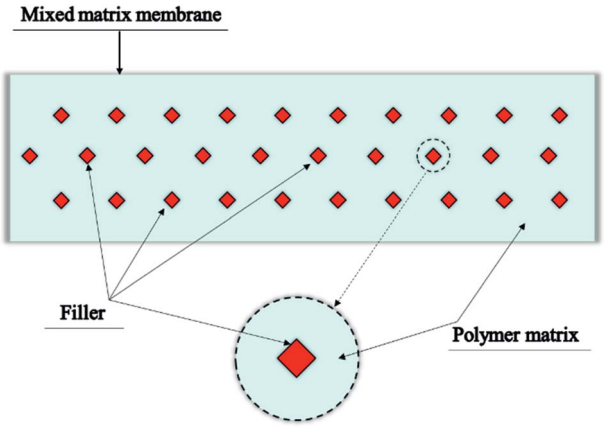

Fig. 1 Schematic illustration of a mixed matrix membrane. Modified and reproduced with permission from ref. 13. Copyright 2010, Elsevier B.V.

Besides, it is also hopeful that MMMs could adapt to the existing matured technology for polymer membrane fabrication, avoiding the massive cost in upgrading existing membrane production equipment, as well as the difficulties, high cost and arduous amplification in fabricating crystalline membranes.[18–20] For these reasons, MMMs may not only improve the separation performance of pure polymer membranes that can be applied in industrial separation in the near future but also be an effective way for new porous materials with good performance but high cost to be used in practical applications, such as metal–organic frameworks (MOFs) and covalent organic frameworks (COFs).

However, although a large number of MMMs for CO_2 separation have been reported, only a few exhibited simultaneously improved permeability and selectivity (separation factor) compared with the corresponding pure polymer membranes. One reason may be the deficiencies of fillers in diffusion or adsorption properties. For example, the incorporation of mesoporous silica with poor adsorption selectivity for CO_2 usually leads to an obvious enhancement in CO_2 permeability, while maintaining or decreasing the CO_2 selectivity compared to the pristine polymer membranes.[21–23] Nik *et al.*[24] compared UiO-66 with its amine functionalized counterpart in enhancing the CO_2/CH_4 separation performance of the 6FDA-ODA polyimide membrane. MMMs prepared with UiO-66 significantly increases the CO_2 permeability compared with the neat 6FDA-ODA membrane without any loss in ideal selectivity, while the incorporation of more CO_2 selective UiO-66-NH_2 can increase both the ideal selectivity and CO_2 permeability of the 6FDA-ODA membrane. These results demonstrate that the design and optimization of properties of fillers are significant in high-performance MMM preparation.

The non-ideality in the morphology of MMMs may be another difficulty that hinders the simultaneous enhancement in selectivity and permeability. Common non-ideal structures include filler particle aggregation, interfacial voids between the filler and polymer phase, polymer chain rigidification around filler particles, and pore blockage on the surface of filler particles, as schematically illustrated in Fig. 2. The aggregation of filler particles may create non-selective voids in the aggregates, and even generate macroscopic defects in the membranes, thus hindering the exploitation of properties of fillers and reducing the selectivity of membranes.[25–27] Interfacial voids between the filler and polymer matrix can form bypasses for gas molecules around the filler particles and also influence the performance of the resulting MMMs.[10,25–30] It is noteworthy that this problem is particularly significant for inorganic fillers such as zeolites since they usually have poor compatibility with organic polymers.[31] The rigidification of polymer chains around the filler

Dahuan Liu received his PhD degree in chemical engineering at the Beijing University of Chemical Technology in 2006 under the supervision of Professor Chongli Zhong. Then he joined the group of Professor Chongli Zhong and was appointed professor at the Beijing University of Chemical Technology. His research mainly focuses on materials development for membrane separation and adsorption using a combination of theoretical methods and experiment.

Chongli Zhong studied chemical engineering at the Beijing University of Chemical Technology and received his Ph.D. degree in 1993 under the supervision of Professor Wenchuan Wang. He worked as an assistant professor in Hiroshima University from 1995–1998 and joined the group of Professor J. de Swaan Arons at the Delft University of Technology as a postdoctoral research fellow in 1998. He joined the Beijing University of Chemical Technology and was appointed professor in 1999. He joined Tianjin Polytechnic University in 2018 and was appointed Director of State Key Lab. of Separation Membranes and Membrane Processes. His main research interests are focused on the computational and experimental study of adsorption and membrane separation using nanoporous materials such as MOFs and COFs.

Published on 04 October 2019. Downloaded by Yunnan University on 8/23/2025 5:29:10 PM.

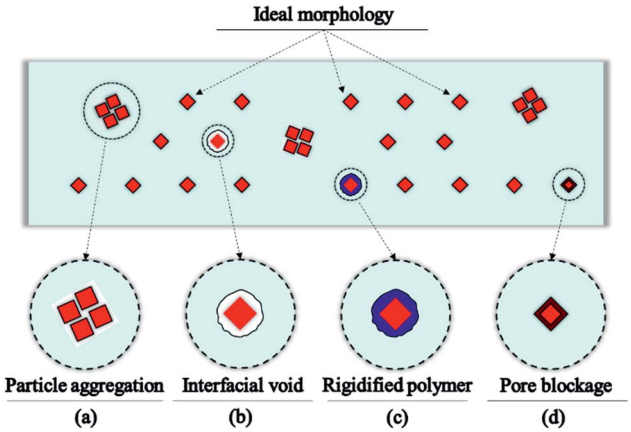

Fig. 2 Schematic illustration of possible non-ideal morphologies of MMMs.

particles may generate a region with less chain mobility and free volume, leading to a permeability reduction.[32,33] Pore blockage by the polymer chains may cause decline in permeability and change the porous filler to be an impermeable one when the pores are plugged completely.[26,34,35] Although in some cases polymer rigidification[36–39] or partial pore blockage[32] can result in desired enhancement in gas selectivity by improving diffusion selectivity, the degree of polymer rigidification or partial pore blockage remains highly difficult to evaluate, characterize, and control. Therefore, polymer rigidification and pore blockage are still commonly considered as two kinds of non-ideal morphologies, rather than strategies for separation performance optimizing.

To solve these problems, various strategies have been proposed to enhance the separation ability of fillers, control the dispersion of filler particles in MMMs, and adjust the interfacial structure between the filler and polymer.[25,31,40–44] Among them, the introduction of a third component into binary MMMs seems to be a promising method. The third component can either be located at the filler–polymer interface, be encapsulated in the pore channels of the filler or distribute in the polymer matrix with the existing filler particles, as shown in Fig. 3, improving the separation performance of MMMs through optimizing membrane morphologies, adjusting filler properties and so on. For example, the third component located at the filler–polymer interface can fill-in the gap or bind the border to eliminate interfacial voids, as schematically illustrated in Fig. 4. This review intends to offer some insights for designing MMMs with an optimized membrane structure and high CO_2 separation performance from a specific point of view of using more than two components in MMMs, although there are some overlaps in the contents with the existing reviews that are mainly focused on binary MMMs.[9–12,14,15,25–27,45–54] The methods for the introduction of the third component, the corresponding physical or chemical changes in the microstructures of MMMs, and the effects on the application of CO_2 separation will be discussed comprehensively, which are classified according to the types of the third component, as shown in Tables S1–S3† (these tables give a summary of the third component incorporation methods, the roles of the third component, and details of the systems studied for each reference). Finally, conclusions and the remaining challenges will be outlined, toward "ternary" MMM fabrication and future research directions.

2 Small molecules as the third component

2.1 Ionic liquids

Ionic liquids (ILs) are molten organic salts that can present in liquid form at low temperatures (usually below 100 °C). In recent years, ILs have attracted much attention in the field of CO_2 capture and separation due to their excellent non-volatility, structural designability and CO_2 solubility. However, the viscous liquid nature and high cost limit their applications in practical separation. Combining ILs with membranes or porous materials may not only avoid the shortcomings of ILs, but also further enhance the CO_2 separation performance of ILs, membranes and porous materials due to the synergistic effect between different components.[55–57] In the field of MMM fabrication, the introduction of ILs may (i) optimize the interfacial interaction and structure between filler particles and the polymer matrix; (ii) regulate the pore structure of fillers; and (iii) enhance the affinity of membranes for CO_2 adsorption, making ILs to be one kind of versatile and effective additive for "ternary" MMMs.

Noble and co-workers first studied the effect of ILs as the third component in MMMs on the CO_2 separation performance of membranes in 2010.[58] "Free" IL was introduced *via* direct blending of zeolite and the polymer matrix. SAPO-34/poly(vinyl-

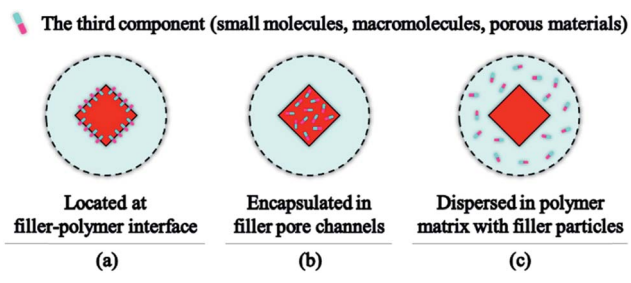

Fig. 3 Schematic illustration of possible existing forms of the third component in ternary MMMs.

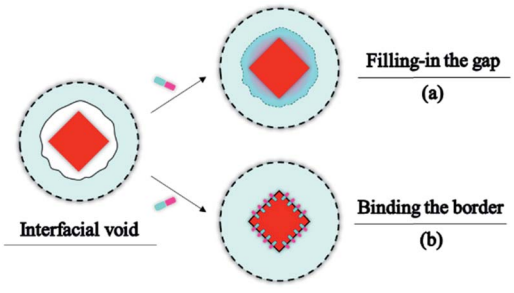

Fig. 4 Schematic illustration of interfacial void healing by the third component.

This journal is © The Royal Society of Chemistry 2019

Published on 04 October 2019. Downloaded by Yunnan University on 8/23/2025 5:29:10 PM.

IL) and SAPO-34/[emim][TF_2N]/poly(vinyl-IL) MMMs were prepared and their CO_2/CH_4 and CO_2/N_2 separation performances were measured. Experimental results show that the CO_2 permeability and CO_2/N_2 selectivity of the three-component membrane are 418% and 25% higher than those of the two-component counterpart, respectively. The introduction of [emim][TF_2N] not only increases the free volume of the membrane, but also strengthens the interaction between SAPO-34 and poly(vinyl-IL) as an interfacial wetting agent, avoiding the formation of interfacial defects. Similarly, Shindo *et al.*[59] introduced [bmim][TF_2N] into a ZSM-5/6FDA–durene system by direct blending. Binary MMMs with only 15 wt% ZSM-5 show largely improved CO_2 permeability but significantly decreased CO_2/CH_4 and CO_2/N_2 selectivity, compared with the pristine 6FDA–durene membrane. The dramatic changes in gas permeability and selectivity are attributed to the interfacial defects between ZSM-5 and 6FDA–durene, which can be healed in the ternary MMM by the addition of ILs. The liquid form IL with good wettability for both the inorganic filler and organic polymer matrix can fill-in the interfacial gaps to eliminate these non-selective voids. With the introduction of 9 wt% IL into such binary MMMs, CO_2/CH_4 and CO_2/N_2 selectivity can be enhanced evidently, even though the CO_2 permeability is decreased. The effects of ILs on improving filler–polymer interface compatibility and eliminating non-selective interfacial voids were also reported in ternary MMMs such as ETS-10/[emim][Ac]/chitosan,[60] SAPO-34/[emim][TF_2N]/PES,[61] ZIF-8/[bmim][NTf_2]/Pebax 1657,[62] and Ag NPs/[bmim][BF_4]/Pebax 1657,[63] alongside their other intrinsic functionalities.

ILs have also been introduced into MMMs *via* confining them in the pores of fillers prior to membrane fabrication, which endows them with special functions in modifying the pore structures and chemical properties of the fillers. For example, Ban *et al.*[64] encapsulated an imidazolium based ionic liquid [bmim][Tf_2N] into the SOD cages of ZIF-8 by *in situ* ionothermal synthesis before the composite was used as the filler in PSF-type MMMs. An obvious cavity-occupying effect of ILs in the cages was observed, which led to a decrease in the effective cage size of ZIF-8 (from 1.12 to 0.59 nm), as illustrated in Fig. 5. The CO_2 adsorption selectivity and molecular sieving effect of ZIF-8 are strongly enhanced with the incorporated IL molecules in the obtained IL@ZIF-8/PSF MMMs. Especially, the CO_2/CH_4 and CO_2/N_2 selectivities at 6 vol% filler loading exhibit 100% and 290% enhancements (from 19.1 to 38.3 and 29.7 to 116), respectively, compared with those of the binary ZIF-8/PSF MMM with the same filler loading.

Li *et al.*[65] also prepared an IL@ZIF-8 composite for MMM fabrication *via* soaking of ZIF-8 in the solution of [bmim][Tf_2N]. Besides the effect of reducing the effective aperture size of ZIF-8 through cavity-occupying, the impregnated IL molecules can be dragged to the outer surface of ZIF-8 nanoparticles during the removal of the solvent. This portion of ILs can interact strongly with PA blocks of Pebax 1657 as well, toughening the filler–polymer interface significantly. Compared with the ZIF-8/Pebax 1657 MMM, the IL@ZIF-8/Pebax 1657 MMM with 15 wt% filler loading shows 78% and 112% higher CO_2/CH_4 and CO_2/N_2 selectivity, respectively. Meanwhile, the mechanical properties

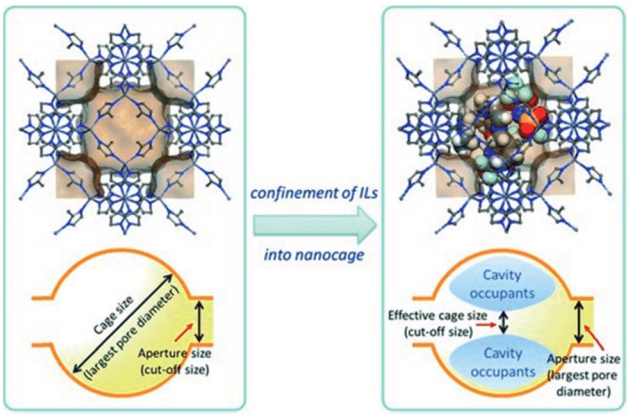

Fig. 5 Schematic illustration of the cavity-occupying concept for tailoring the molecular sieving properties of ZIF-8 by the incorporation of ILs. Reproduced with permission from ref. 64. Copyright 2015, WILEY-VCH Verlag GmbH & Co. KGaA, Weinheim.

are also largely improved (42% enhancement in tensile strength and 226% increase in breaking elongation, compared with the 15 wt% ZIF-8/Pebax 1657 MMM), highlighting the important roles played by ILs as the third component in MMMs.

In our previous work,[66] an amine-containing task-specific IL, [C_3NH_2bim][Tf_2N], was introduced into MMMs by preloading in NH_2-MIL-101(Cr), as shown in Fig. 6. The interactions between IL molecules and the coordinative unsaturated Cr(III) metal centre avoided the leakage of the IL from the framework during membrane fabrication. The amine-containing IL molecules in the MMMs can strongly enhance the CO_2 affinity of membranes and act as facilitated transport carriers for CO_2 molecules, resulting in a crowding-out effect for N_2. Compared with the binary MMM with 5 wt% filler loading, the IL-containing MMM exhibits a significant reduction in N_2 permeability while with only a slight decrease in CO_2 permeability, leading to a 112% enhancement in the ideal CO_2/N_2 selectivity.

Another method for introducing ILs into MMMs is to modify the filler surface with ILs. For example, Lin *et al.*[67] decorated the surface of HKUST-1 particles with [emim][Tf_2N]. An IL layer was formed on the outer surface of filler particles and acted as an interfacial binder between HKUST-1 and the 6FDA–durene

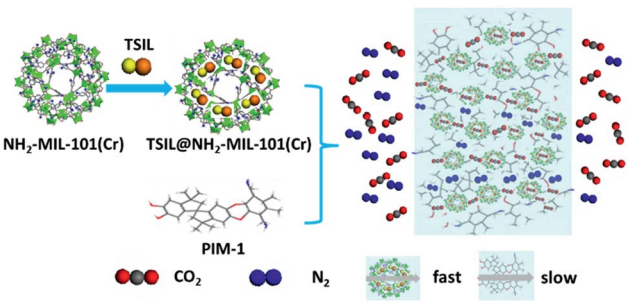

Fig. 6 Illustration of the preparation of the TSIL@NH_2-MIL-101(Cr)/PIM-1 MMMs, and the gas separation process.

Published on 04 October 2019. Downloaded by Yunnan University on 8/23/2025 5:29:10 PM.

polymer. The formation of nonselective interfacial voids was successfully restricted, leading to an increase in CO_2 selectivity compared with the MMM using undecorated HKUST-1 as the filler. Ahmad *et al.*[68] modified SAPO-34 with [emim][Tf_2N] through a simple immersion method. The negatively charged zeolite surface can form electrostatic interactions with the cation of the IL, thus adsorbing IL molecules on the surface of SAPO-34. The adsorbed IL molecules can eliminate interfacial voids by improving the interfacial adhesion between inorganic SAPO-34 and the organic PSF matrix. The CO_2 solubility was also increased, leading to simultaneous improvements in CO_2 permeability and selectivity. Through an epoxide ring-opening reaction, Huang *et al.*[69] covalently modified the surface of GO nanosheets with an amine-terminated IL, 1-(3-aminopropyl)-3-methylimidazolium bromide. Interfacial interactions and compatibility between GO laminates and the Pebax 1657 matrix are improved upon IL modification, and the introduced amine groups can facilitate CO_2 transport through reversible reactions at the same time. Owing to these effects of the introduced IL, the CO_2 permeability, as well as CO_2/N_2 and CO_2/H_2 selectivity of the IL-GO/Pebax 1657 MMM with 0.2 wt% filler loading exhibits simultaneously enhancement compared with the pure Pebax 1657 membrane and the GO/Pebax 1657 MMM with the same filler loading. The covalent functionalization of the surface of zeolite 4A with [APTMS][Ac] also eliminated the interfacial voids and increased CO_2 solubility of zeolite 4A/PSF MMMs.[70]

Besides, the polymer matrix can also be treated with ILs prior to the fabrication of MMMs to obtain better compatibility at the filler–polymer interface. For example, Jomekian *et al.*[71] pre-treated Pebax 1657 with [DnBM][Cl]. The IL modification enhanced the interactions of Pebax 1657 with the ZIF-8 filler, resulting in higher ideal selectivities of CO_2/CH_4, CO_2/N_2, and CO_2/H_2 than their unmodified counterparts. Ahmad *et al.*[72] introduced [bmim][Ac] as the third component for the SAPO-34/PSF asymmetric MMMs through post-impregnation of MMMs in ethanol solution of ILs. They found that the IL molecules could diffuse to the filler–polymer interface to seal the non-selective voids, thus greatly improving the CO_2/N_2 selectivity of the original MMMs.

2.2 Organic silanes

Organic silanes contain silanoxyl groups that are reactive to inorganic substances and organic functional groups that are reactive or compatible with organic substances. Thus, they can enhance the interaction or compatibility between inorganic and organic substances. Owing to this characteristic, organic silanes have been introduced through filler modification in some studies to optimize the interfacial interactions and structures between the filler and polymer matrix in MMMs. In addition, the functional groups in organic silanes can also improve the affinity of CO_2.

Li *et al.*[33] first functionalized zeolite 4A with 3-aminopropyldiethoxymethylsilane (APDEMS) prior to MMM fabrication. APDEMS was anchored on the surface of zeolite through covalent bonds between the hydrolyzed silanols and –OH groups. An effect of decreasing partial pore blockage of zeolite by PES chains was discovered due to the additional space brought about by the molecular chains of APDEMS on the zeolite surface. Benefiting from this, slight improvements in CO_2 permeability and CO_2/CH_4 selectivity were observed.

Zhu *et al.*[73] modified MIL-53(Al) with 3-aminopropyltrimethoxysilane (APTMS) and incorporated the functionalized MOF particles into Ultem® 1000 for the fabrication of asymmetric MMMs, as shown in Fig. 7. The hydrogen bonds between the amine groups from APTMS and the polymer chains can enhance the affinity of MOF particles to the polymer matrix and reduce filler agglomeration and interfacial voids. Meanwhile, the dipole–quadrupole interaction between amine groups and CO_2 molecules can improve CO_2 adsorption and crowd out N_2 molecules. As a result, the obtained MMM with modified MIL-53(Al) (10 wt% loading) shows a 68% enhancement in CO_2/N_2 selectivity without sacrificing CO_2 permeance compared with the MMM based on unmodified MIL-53(Al).

Interestingly, organic silane is observed to be able to change the oriented arrangement of the 2D filler in MMMs.[74] In the work of Qiao *et al.*, stretched polyvinylamine acid chains grafted on a hydroxylated PSF substrate acted as the orientation guide for Na-exchanged montmorillonite (MT), while the APTES molecules served as crossbeams that connect MT and polymer chains, as shown in Fig. 8. Since the interlayer gaps in MT can be considered as high-speed transport channels for CO_2 molecules, the MMMs containing vertically aligned MT were found to have about 80% higher CO_2 permeance than the MMMs containing randomly arranged MT due to the largely shortened transport path.

Recently, Shamsabadi *et al.*[75] functionalized the surface of TiO_2 nanoparticles using APDEMS. The interactions between TiO_2 and Pebax 1657, as well as the CO_2 affinity of the membrane, are enhanced because of the introduced amine groups from APDEMS. Amedi *et al.*[76] modified the ZIF-8 surface with 3-aminopropyltriethoxysilane (APTES), which exhibits positive effects on improving filler–polymer interface compatibility and separation performance of ZIF-8/Pebax 1657 MMMs. This kind of organic silane was also used to enhance the GO and Pebax 1657 interfacial compatibility by grafting on GO nanosheets and also provided amine groups as CO_2 facilitated transport carriers.[77]

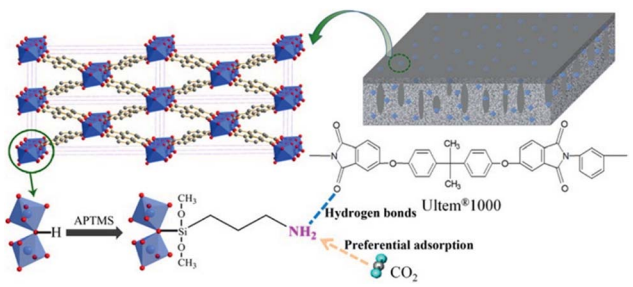

Fig. 7 Structure of APTMS-MIL-53(Al)/Ultem® 1000 asymmetric MMMs, the post-synthetic modification of MIL-53 by the condensation reaction, and the functions of APTMS in MMMs. Reproduced with permission from ref. 73. Copyright 2016, American Chemical Society.

 This journal is © The Royal Society of Chemistry 2019

Published on 04 October 2019. Downloaded by Yunnan University on 8/23/2025 5:29:10 PM.

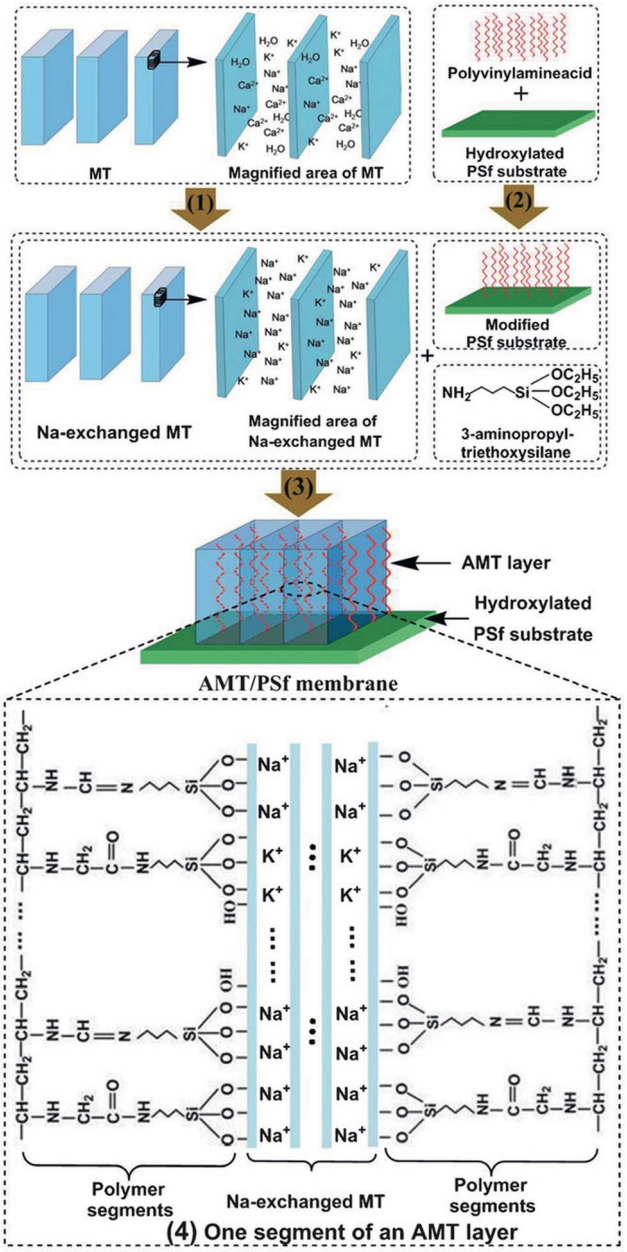

Fig. 8 Formation process and the proposed construction of the AMT/PSF membrane. Reproduced with permission from ref. 74. Copyright 2016, WILEY-VCH Verlag GmbH & Co. KGaA, Weinheim.

2.3 Metal ions

As known, CO_2 molecules may form reversible π-complexation with some metal ions, leading to preferential adsorption and facilitated transport of CO_2. Thus, metal ions have been considered as the third component in MMMs to enhance the CO_2 separation performance of membranes.

Li *et al.*[78] introduced Zn^{2+} as the third component into the POSS® octa amic acid/Matrimid® 5218 MMMs for CO_2 separation through post-impregnation of MMMs in methanol solution of $ZnCl_2$. On one hand, the binding of Zn^{2+} onto the particles can narrow the pore size to introduce a size exclusion effect in these MMMs. On the other hand, the reversible complexion of CO_2 molecules with Zn^{2+} can facilitate the transport of CO_2 molecules. Therefore, the CO_2 diffusion selectivity was increased, leading to a significant improvement in CO_2/CH_4 selectivity (from 37.2 to 62.8). The chelating of Ag^+ on the PDA NPs can also facilitate CO_2 transport to improve the CO_2 permeability and CO_2/CH_4 selectivity of PDA NPs/Pebax 1657 MMMs.[79]

Metal ions have also been introduced into MMMs through partial ion substitution of fillers. For example, partial substitution of Zn^{2+} with Co^{2+} in ZIF-108 can increase the pore size and CO_2 adsorption selectivity of ZIF-108, contributing to the simultaneous improvement of CO_2 permeability and CO_2/gas selectivity of the corresponding PSF-based MMMs.[80] Partial substitution of Zr with Ti^{4+} in the UiO-66 framework can enhance the CO_2 affinity of UiO-66, thus improving the CO_2 permeability of the UiO-66/PIM-1 MMMs.[81]

Wang *et al.*[82] designed two kinds of MMMs containing CO_2 facilitated transport pathways by using PVI@CNT and Zn^{2+}-PVI@CNT as fillers in Matrimid® 5218, respectively. The imidazole groups in the latter were covered by the chelated Zn ions, inducing distinct CO_2 separation performance at dry and humid states in these two kinds of MMMs. Under dry conditions, the MMMs containing Zn ions have evident improvement in CO_2 separation performance compared with the MMMs incorporated with the pristine CNT, while the CO_2 separation performance of PVI@CNT containing MMMs remains almost unchanged. Under humid conditions, the opposite phenomenon was observed. These results demonstrate that the reversible π-complexation (as shown in Fig. 9) between CO_2 molecules and Zn ions can promote the transport of CO_2. Moreover, in contrast to the N-containing functional groups, the facilitated transport effect of Zn ions can easily be deactivated because of the stronger binding force of Zn ions with water molecules than CO_2 molecules. In their successive work, four different metal ions (Cu^{2+}, Fe^{2+}, Ca^{2+} and Mg^{2+}) were compared as the third component in PVI@CNT/Matrimid® 5218 MMMs. The introduction of transition metal ions (Cu^{2+} and Fe^{2+}) can serve as CO_2 facilitated transport carriers and increase the permeability of CO_2, while the employment of main-group metal ions (Ca^{2+} and Mg^{2+}) cannot facilitate the transport of CO_2 due to their simple electron orbitals for which it is harder to form

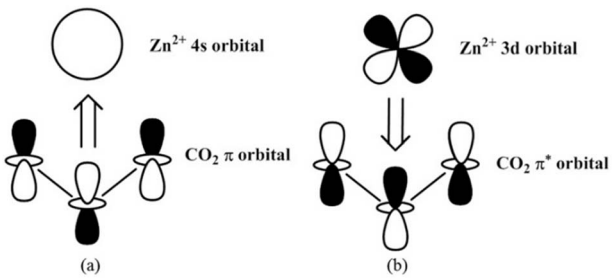

Fig. 9 The mechanism diagram for reversible interactions between Zn^{2+} and CO_2 (a) σ-bonding and (b) π-bonding. Reproduced with permission from ref. 84. Copyright 2016, Elsevier B.V.

Published on 04 October 2019. Downloaded by Yunnan University on 8/23/2025 5:29:10 PM.

coordination compounds with CO_2.[83] A similar CO_2 facilitated transport effect of metal ions was also found in the studies about Zn^{2+}–PDA–GO/Pebax 1657 MMMs.[84]

Recently, Zhang *et al.*[85] *in situ* synthesized bimetallic ZIF-8 (Ni/Zn = 1/12) and then incorporated it into Pebax 2533. Compared with Zn-ZIF-8, the Ni/Zn-ZIF-8 based MMMs exhibit enhanced CO_2 permeability and CO_2/N_2 selectivity due to the improved CO_2 affinity of the filler by Ni ions. These studies demonstrate the potential applications of metal ions in optimizing the separation performance of MMMs.

2.4 Other small molecules

Besides ILs, organic silanes and metal ions, other types of small molecules with complex structures and functionalities have also been added to binary MMMs by both physical and chemical methods.

Through physical blending, Cakal *et al.*[86] introduced 10 wt% 2-hydroxy 5-methyl aniline (HMA) into SAPO-34/PES MMMs. Besides the effect of eliminating interfacial voids, the introduction of HMA also can reduce the CO_2 permeability and increase the CO_2/CH_4 selectivity *via* stiffening the polymer matrix like an anti-plasticizer. In the ZSM-5/liquid sulfolane/6FDA–durene MMMs,[87] the liquid sulfolane can prevent the formation of nonselective interfacial voids between the inorganic filler and organic polymer matrix through gap-filling owing to its liquid nature and good wettability for both the filler and polymer matrix, thus improving the CO_2/gas selectivity obviously. Nasir *et al.*[88] introduced 15 wt% diethanolamine (DEA) into a carbon molecular sieve (CMS)/PES MMM containing 30 wt% CMS. DEA can increase the CO_2 solubility significantly and act as facilitated transport carriers for CO_2 due to the reversible CO_2-amine reaction. Therefore, the CMS/DEA/PES membrane exhibits a 139% higher CO_2 permeability and 363% higher CO_2/CH_4 ideal selectivity than the CMS/PES membrane at 25 °C and 1.0 MPa. Blending ethylenediamine (EDA) into the ZIF-90/Matrimid® 5218 MMMs can lead to further covalent bonding between the filler and polymer due to the reactivity of EDA with the aldehyde groups from the linker of ZIF-90 and polymer chains of Matrimid® 5218.[89] The linker distortion and polymer chain mobility were suppressed at the filler–polymer interface because of the covalent bonding, leading to the reduction in the effective pore size and stiffness in the polymer matrix to some extent. As a result, the H_2/CO_2 diffusion selectivity of MMMs was significantly improved, as well as the H_2/CO_2 separation factor. The inclusion of glycerol triacetate (GTA) into the MWCNT-NH_2/Pebax 1657 MMMs can promote the dispersion of CNTs in the matrix by increasing the hydrophilicity of CNTs *via* GTA adsorption on the filler surface.[90] GTA can also increase the chain mobility and fractional free volume of the membrane like a plasticizer, leading to a great improvement in CO_2 permeability but decreases in CO_2/CH_4 and CO_2/N_2 selectivities.

To improve the blending efficiency, a new "ship-in-a-bottle" strategy was proposed by Amooghin *et al.*[91] to encapsulate a Co^{2+}–diamine–diketone complex in zeolite Y. The effect of the introduced Co-complex on the CO_2/CH_4 separation performance of zeolite Y/Matrimid® 5218 MMMs was investigated. On one hand, the presence of the Co-complex in the pores can narrow the effective pore size of the zeolite and decrease the gas permeabilities of membranes, especially the CH_4 permeability due to the relatively large molecular size of CH_4. On the other hand, the N-containing complex can act as a Lewis base and facilitate the transport of CO_2 as a Lewis acid, through weak acid–base interactions. The combination of these two effects results in an evident increase (158% compared with the zeolite Y/Matrimid® 5218 MMM) in CO_2/CH_4 selectivity and a slight improvement in CO_2 permeability of the corresponding MMM with 15 wt% filler loading.

Through chemical routes, GO nanosheets have been modified with EDA molecules before being incorporated into the Ultem® 1000 matrix.[92] It is found that the introduced EDA molecules can increase filler–polymer interfacial interactions, improve the CO_2 affinity of membranes, and act as CO_2 transport carriers in MMMs. As a result, a greatly improved CO_2/CH_4 selectivity was achieved in GO/Ultem® 1000 MMMs with 0.75 wt% GO loading (from 58.4 to 142.7). Venna *et al.*[93] utilized phenyl acetyl, decanoyl acetyl, and succinic acid groups to functionalize the external surface of UiO-66-NH_2 particles. These organic moieties can tune the interactions between UiO-66-NH_2 and the polymer (Matrimid® 5218), affecting the interfacial microstructures and separation performance of the corresponding MMMs.

Especially, Gao *et al.*[94] covalently attached *cis*-5-norbornene-*exo*-2,3-dicarboxylic anhydride (ND) molecules on the surface of UiO-66-NH_2 particles, which further participate in the ring-opening metathesis polymerization (ROMP) of norbornene (NB) for the fabrication of poly(NB/MOF-ND) MMMs, as shown in Fig. 10. The grafted ND molecules serve as connecting bridges of the two phases. Owing to the strong covalent interaction between the MOF and polymer, the MMM with 20 wt% filler loading exhibits exceptional improvement in mechanical toughness (105% in tensile strength compared with the pristine polynorbornene membrane). The H_2/CO_2 selectivity was also improved compared with the pristine polynorbornene membrane.

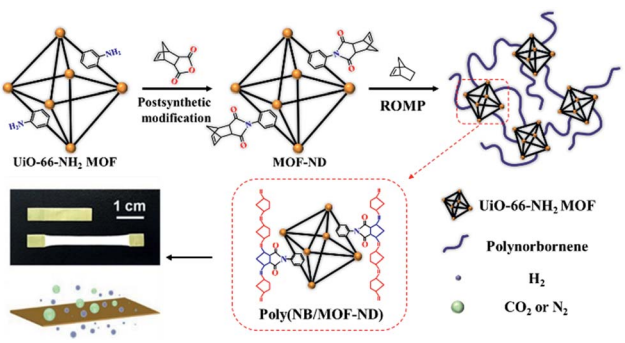

Fig. 10 Postsynthetic modification and covalent attachment of UiO-66-NH_2 in the polynorbornene matrix by ROMP and a photo reflecting the toughness and molecular sieving properties of the resulting MMMs. Modified and reproduced with permission from ref. 94. Copyright 2018, American Chemical Society.

 This journal is © The Royal Society of Chemistry 2019

Published on 04 October 2019. Downloaded by Yunnan University on 8/23/2025 5:29:10 PM.

Another interesting study is the construction of rigid and connected paths between UiO-66-NH_2 and PIM-1 in MMMs by 4-cyanobenzoyl chloride through covalent crosslinking.[95] As shown in Fig. 11, the diffusion of gas molecules from the polymer zone to the MOF channels can be greatly enhanced by the rigid paths instead of randomly packed polymer chains that may block the surface pores of MOF particles. At the same time, preferential concentrated CO_2 molecules because of rich adsorption sites and high porosity can crowd out N_2 molecules from UiO-66-CN pores. As a result, the CO_2 permeability and CO_2/N_2 selectivity of UiO-66-NH_2/PIM-1 MMMs were increased significantly with the introduction of 4-cyanobenzoyl chloride, especially for mixed-gas separation.

3 Macromolecules as the third component

Compared to small molecules, macromolecules have long molecular chains, abundant functional groups, and good compatibility with the polymer matrix, which may endow them with special advantages in filling the gaps between the filler and polymer matrix, introducing a large amount of CO_2-philic functional groups into MMMs, or bridging the filler and polymer matrix through covalent or noncovalent interactions. So far, commonly used macromolecules include polyethylene glycol (PEG) and its derivatives, polydopamine (PDA), polyethyleneimine (PEI) and some other polymers.

3.1 PEG

PEG is low molecular weight (200–20 000) polyethylene oxide (PEO) synthesized through ring-opening polymerization of ethylene oxide. Due to the good compatibility with many substances and good solubility in water and many organic solvents, PEG can be used as a dispersant and stabilizer for insoluble solid particles in suspensions. Moreover, the formation of dipole–quadrupole interactions between polar ethylene oxide (EO) units and CO_2 molecules endows PEG with excellent CO_2 affinity. Therefore, PEG and its derivatives have been frequently used as an additional additive in the fabrication of MMMs for CO_2 separation. For example, blending 5 wt% PEG 200 into 5 wt% ZSM-5/Matrimid® 5218 MMM can eliminate filler–polymer interfacial voids and enhance CO_2 affinity of the membrane, thus increasing the CO_2 permeability and CO_2/CH_4 selectivity by 33% and 11%, respectively.[96] Similar phenomena were observed in ZIF-8/Matrimid® 5218 MMMs.[97] It has also been reported that the addition of PEG 200 can increase the fractional free volume of NaX/Pebax 1657 MMMs, contributing to the increase in gas permeability.[98]

Besides physical blending, PEG was also applied to be chemically grafted on the filler in MMMs.[92,99–104] For example, Roh *et al.*[101] prepared dual-functionalized mesoporous TiO_2 hollow nanospheres (f-MTHS) for MMM fabrication through successive modification with APTMS and poly(ethylene glycol) diglycidyl ether (PEGDE). PVC-*g*-POEM, an amphiphilic graft copolymer consisting of poly(vinyl chloride) (PVC) main chains and poly(oxyethylene methacrylate) (POEM) side chains, was used as the polymer matrix. Pristine TiO_2 is an inorganic material that does not have specific interactions with CO_2 and good compatibility with the organic polymer. Therefore, the incorporation of 20 wt% unmodified MTHS into PVC-*g*-POEM causes an increase in CO_2 permeability but a reduction in CO_2/N_2 selectivity. In contrast, the membrane containing the same loading of f-MTHS exhibits simultaneously improved CO_2 permeability and CO_2/N_2 selectivity. The improved interfacial contact between TiO_2 and PVC-*g*-POEM due to the grafted PEG chains, as well as the facilitated CO_2 transport by the EO groups in PEG and the amine groups from APTMS, is demonstrated to have made important contributions in the separation process.

Li *et al.*[102] modified GO nanosheets with poly(ethylene glycol) monomethyl ether (PEGME, M_w = 5000). Compared with the membrane incorporated with 10 wt% pristine GO, the

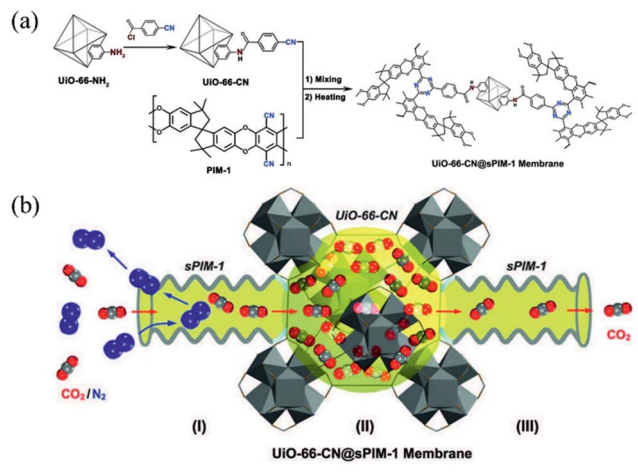

Fig. 11 (a) Synthesis diagram of the preparation of the UiO-66-CN@sPIM-1 hybrid membrane. (b) CO_2 and N_2 transport across the UiO-66-CN/sPIM-1 membrane. Reproduced with permission from ref. 95. Copyright 2019, WILEY-VCH Verlag GmbH & Co. KGaA, Weinheim.

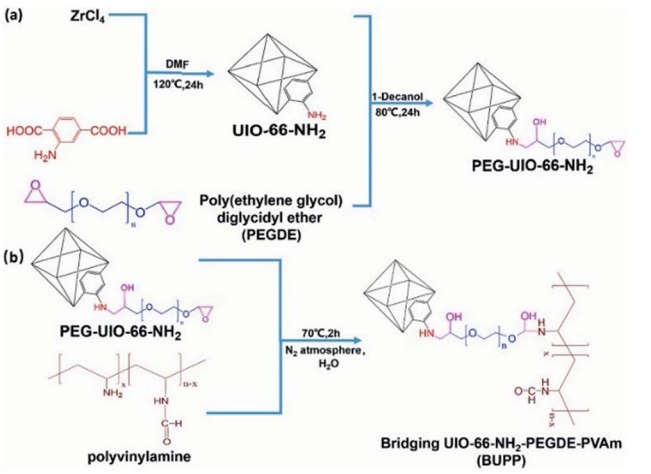

Fig. 12 (a) The synthesis route of PEG–UiO-66-NH_2 nanoparticles. (b) The synthesis route of BUPP. Reproduced with permission from ref. 104. Copyright 2018, Elsevier B.V.

Published on 04 October 2019. Downloaded by Yunnan University on 8/23/2025 5:29:10 PM.

membrane containing the same loading of PEG-modified GO shows an increase of over 180% in CO_2 permeability because of the enhanced CO_2 affinity and facilitated CO_2 transport effects of the EO groups. Xie *et al.*[103] developed well-defined core–shell MOF nanoparticles by chemical coating UiO-66-NH_2 with a PEG-based shell. Embedding the core–shell MOF nanoparticles into the polyactive membrane results in a significant increase in CO_2/N_2 selectivity (from 2.1 to 47) compared with the UiO-66-NH_2/polyactive MMM with 20 wt% filler loading. The poor selectivity of the UiO-66-NH_2/polyactive MMM may be attributed to the nonselective defects in the membrane induced by the agglomeration of filler particles and incompatibility between the filler and polymer matrix, which can be effectively eliminated by coating of the PEG-based shell. Moreover, the PEG-based shell can selectively block the diffusion of N_2 molecules through the MOF core, resulting in the increase in CO_2/N_2 selectivity.

Especially, Xu *et al.*[104] bridged the UiO-66-NH_2 nanoparticles and the polyvinylamine (PVAm) polymer with PEGDE through a two-step chemical crosslinking process, as shown in Fig. 12. The MMM cast with the solution of bridging UiO-66-NH_2–PEGDE–PVAm (BUPP) on the PSF substrate displays better CO_2/N_2 separation performance than the MMM prepared by simply blending UiO-66-NH_2 into the PVAm matrix with the same filler loading (28.5 wt%). The bridging between filler–filler and filler–polymer is believed to be able to suppress the formation of nonselective interfacial voids in MMMs.

3.2 PDA

During the self-polymerization of dopamine, a dense and adhesive PDA coating layer can form on the surface of various substances through the formation of strong covalent and non-covalent bonds with surfaces. This property of dopamine has been applied in the fabrication of MOF membranes to enhance the compatibility and cohesion between the MOF layer and the substrates[105–107] and heal the tiny defects in the MOF layer.[108] It is easy to imagine that PDA can also be used to improve the compatibility and adhesion between two different phases (disperse phase and continue phase).

Wang *et al.*[109] coated nanosized ZIF-8 particles with an ultrathin PDA layer (about 1–2 nm in thickness) to optimize the interfacial microstructure of ZIF-8/TBDA2-6FDA-PI MMMs. Hydrogen bonds between the abundant secondary or primary amine groups from the PDA layer and the tertiary amine from the TB-based TBDA2-6FDA polymer can benefit the interfacial compatibility between ZIF-8 and the PI matrix, as schematically shown in Fig. 13. As a result, a denser and more integrated morphology was observed in the cross-sectional SEM images of PDA@ZIF-8/PI MMMs instead of the counterparts containing pristine ZIF-8 nanoparticles. Although the CO_2 permeability of PDA@ZIF-8/PI MMMs (1056 barrer at 30 wt% filler loading) is slightly lower than that of ZIF-8/PI MMMs (1437 barrer), it still has a significant improvement compared with that of the neat PI membrane (285 barrer). Besides, the PDA containing MMMs have higher CO_2 selectivities than their counterparts. These results indicate that the PDA layer will not significantly affect the pores on the surface of ZIF-8 while effectively eliminating the formation of undesirable voids at the filler–polymer interface. Similarly, Dong *et al.*[110] used PDA-coated ZIF-8 as the filler to prepare MMMs. They found that the PDA layer can not only mitigate the interfacial defects between ZIF-8 and Pebax 4033, but also facilitate CO_2 transport through interactions between CO_2 molecules and abundant –OH and amino groups in PDA. Compared with the 15 wt% ZIF-8/Pebax 4033 membrane, the MMM containing the same loading of PDA@ZIF-8 exhibits increases of 30% and 25% in CO_2 permeability and CO_2/N_2 ideal selectivity, respectively. In addition, the PDA coating method has been adopted in the fabrication of MMMs for other applications, such as PDA@MIL-101(Cr)-SO_3H/PVA MMMs for pervaporation dehydration of ethylene glycol in our previous work,[111] PDA@CNT/SPEEK proton exchange MMMs for

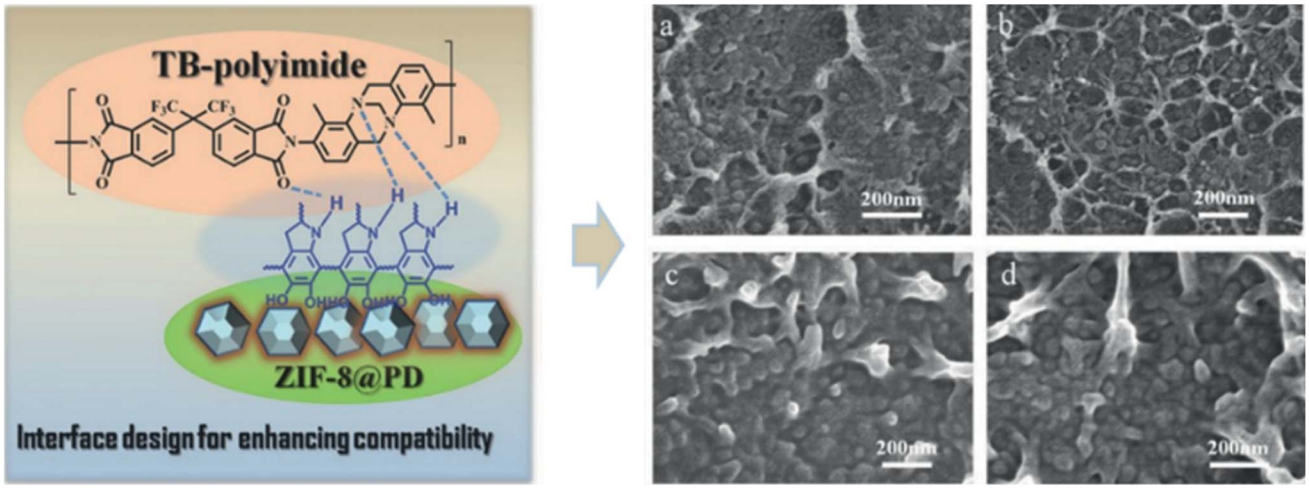

Fig. 13 Schematic illustration for interface design of the PDA@ZIF-8/PI MMM and the cross-sectional microstructure of (a) ZIF-8/PI (20 wt%), (b) ZIF-8/PI (30 wt%), (c) PDA@ZIF-8/PI (20 wt%), and (d) PDA@ZIF-8/PI (30 wt%). Reproduced with permission from ref. 109. Copyright 2016, WILEY-VCH Verlag GmbH & Co. KGaA, Weinheim.

 This journal is © The Royal Society of Chemistry 2019

Published on 04 October 2019. Downloaded by Yunnan University on 8/23/2025 5:29:10 PM.

vanadium flow batteries,[112] and O_2 selective PDA@CAU-1-NH_2/PMMA MMMs for Li–air batteries.[113]

It should be mentioned that the PDA layer on the filler surfaces also provides a versatile platform for secondary modifications. For example, as discussed in the previous section (Section 2.3), Zn ions can be chelated on the GO nanosheets with the aid of PDA coating to improve the separation performance of MMMs.[84] PDA-assisted co-deposition or grafting of polyethyleneimine (PEI) on the filler surface has also been reported,[114–116] which will be discussed in the following section.

3.3 PEI

PEI is a polymer with repeating units composed of an amine group and two methylene spacers. Branched PEIs contain a large amount of primary, secondary and tertiary amino groups that have a strong affinity to CO_2 molecules. Thus, they have been frequently impregnated in porous materials to enhance their adsorption capacity and selectivity to CO_2.[117–121] For example, Xu *et al.*[117] prepared PEI-modified MCM-41 through a wet impregnation method. The strong interaction between CO_2 and the numerous amino groups from PEI can turn the composite adsorbent into a "CO_2 molecular basket" for "packing" CO_2 in a condensed form in nanoporous channels.

One way to introduce PEI into binary MMMs is adopting PEI-impregnated porous materials as the filler. Wu *et al.*[122] modified mesoporous MCM-41 with PEI through impregnation. The amount of PEI in the composite was estimated to be about 50 wt%. Despite the reduction in the actual weight percentage of porous MCM-41, the membrane incorporated with 20 wt% composite filler exhibits a higher increase in CO_2 permeability (157%) than the counterpart containing 20 wt% pristine MCM-41, compared with the pure Pebax 1657 membrane. This phenomenon fully demonstrates the facilitated transport effect of PEI on CO_2 molecules. The CO_2/CH_4 and CO_2/N_2 selectivity were also significantly improved because of the enhanced CO_2 adsorption. Xin *et al.*[123] immobilized PEI into MIL-101(Cr) *via* a vacuum-assisted wet impregnation method. The reaction between amine groups and the Lewis acid centre (coordinative unsaturated Cr sites) reduced the leakage and helped in the uniform distribution of PEI.[124,125] The PEI chains on the surface of MIL-101(Cr) can improve the filler–polymer compatibility because of the electrostatic interaction and hydrogen bonds between amine groups in PEI and sulfonic acid groups in SPEEK. In the PEI-MIL-101(Cr)/SPEEK MMMs, the CO_2 molecules can penetrate the membrane quickly through the facilitated transport channels formed by PEI-modified MIL-101(Cr), while the CH_4 or N_2 molecules can only transport slowly through the polymer matrix, as shown in Fig. 14. Therefore, the CO_2 permeability and the CO_2/CH_4 and CO_2/N_2 selectivity of 40 wt% PEI-MIL-101(Cr)/SPEEK MMM are much higher than that of the 40 wt% MIL-101(Cr)/SPEEK MMM.

Grafting PEI chains onto the surface of filler materials is another way to introduce PEI into MMMs. As we mentioned above, PEI can be co-deposited or grafted on the surface of TiO_2 (ref. 114 and 116) and SiO_2 (ref. 115) with the assistance of PDA. All the MMMs incorporated with these modified fillers exhibit

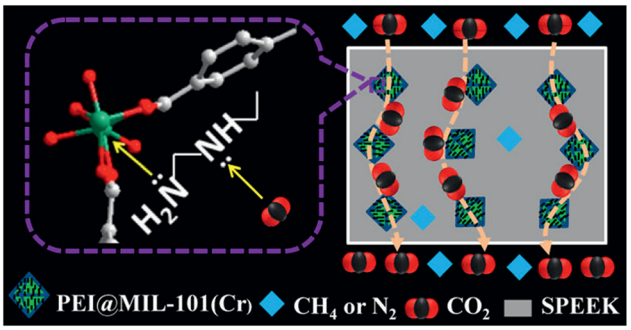

Fig. 14 Facilitated transport mechanism of CO_2 in PEI@MIL-101(Cr)/SPEEK MMMs. Reproduced with permission from ref. 123. Copyright 2015, American Chemical Society.

improved CO_2 separation performance compared with the MMMs containing pristine TiO_2 or SiO_2, benefiting from the filler–polymer interfacial compatibility optimization effect and CO_2 facilitated transport effect of both PDA and PEI.

Li *et al.*[102] incorporated PEI-modified GO nanosheets into Pebax 1657 to improve the CO_2 separation performance. Compared with the MMM incorporated with 10 wt% pristine GO, the MMM containing the same loading of PEI-modified GO has an increase of over 320% (from 255 to 1090 barrer) in CO_2 permeability. The CO_2/CH_4 and CO_2/N_2 selectivities are also improved from 25 to 32 and 59 to 104, respectively. These increases are mainly because of the enhanced CO_2 affinity and facilitated CO_2 transport effects of the amine groups in PEI. It is worth mentioning that PEG and PEI dual-functionalization of GO nanosheets can further enhanced the CO_2 separation performance by combining the favourable effects of PEG and PEI simultaneously in one membrane.

In our previous work,[126] CAU-1 nanoparticles were grafted with PEI through glutaraldehyde bridging and then incorporated into a crosslinked poly(ethylene oxide) (XLPEO) rubbery polymer. Schematic illustrations of the surface functionalization of CAU-1 with PEI and the proposed effects of the grafted PEI on MMMs are shown in Fig. 15. The dispersity of CAU-1 nanoparticles in the pre-crosslinking suspension MMMs was greatly improved after surface modification with PEI chains, thus effectively eliminating the formation of large aggregates and the accompanying nonselective voids in MMMs. Moreover, the PEI chains stretched in the polymer matrix can direct the CO_2 molecules to transport through MOF channels, thus helping the exploitation of the separation ability of the filler material. 30 wt% CAU-1/XLPEO exhibits a dramatic increase in CO_2 permeability and decrease in CO_2/CH_4 selectivity due to the microvoids caused by filler agglomeration. In contrast, both the CO_2 permeability and CO_2/CH_4 selectivity in PEI–CAU-1/XLPEO MMMs increase steadily even when the filler loading is up to 30 wt%.

Gao *et al.*[127] prepared PEI-grafted ZIF-8 *via in situ* grafting modification during the room-temperature synthesis of ZIF-8. Excepting for the effect in improving filler–polymer compatibility, it is demonstrated that the *in situ* grafting of PEI can also increase the porous properties (BET surface area, total pore

Published on 04 October 2019. Downloaded by Yunnan University on 8/23/2025 5:29:10 PM.

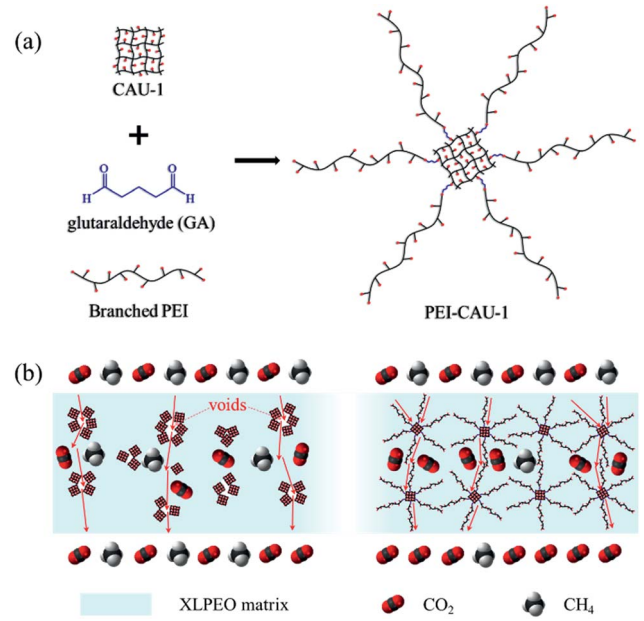

Fig. 15 (a) Schematic illustrations of the surface functionalization of CAU-1 with PEI. (b) Proposed gas permeation process in CAU-1 and PEI–CAU-1 based MMMs. Reproduced with permission from ref. 126. Copyright 2018, Elsevier B.V.

volume, and micropore diameter) and CO_2 adsorption ability of ZIF-8, making PEI-*g*-ZIF-8 a more suitable filler in MMMs to enhance CO_2 separation performance.

Through the covalent linkages or hydrogen bonds between PEI and the terminal –CHO and $-NH_2$ groups on the outer surface of filler particles, Cheng *et al.*[128] externally functionalized a three-dimensional covalent organic framework (COF), COF-300, with PEI to further enhance the CO_2 separation performance of COF-300 based MMMs. The filler–polymer interactions are strengthened due to the hydrogen bonds between PEI and the 6FDA-DAM and Pebax 1657 polymers, leading to the increase in CO_2 selectivity and slight decrease in CO_2 permeability by rigidifying the polymer chains around the filler.

3.4 Other macromolecules

Besides PEG, PDA and PEI, a variety of polymers have also been applied as the third component to improve the CO_2 separation performance of MMMs from different aspects. For example, polyvinylpyrrolidone (PVP) has been introduced as a stabilizer for Pd nanoparticles to eliminate particle agglomeration in MMMs.[129] The formation of large voids was inhibited and the preferential adsorption ability of Pd nanoparticles was well exploited with a uniform filler distribution, contributing to the improvement in H_2/CO_2 selectivity.

Liu *et al.*[130] prepared a polyzwitterion coated CNT composite, poly(SBMA)@CNT, *via* precipitation polymerization, and incorporated it into the Matrimid® 5218 matrix for MMM fabrication. In the dry state, the preferential affinity of poly(SBMA) toward CO_2 due to the quaternary ammonium in its repeating unit can help improve the CO_2/CH_4 selectivity (from 42.8 to 73.3). Under humid conditions, the strong electrostatic interaction between the introduced poly(SBMA) and water molecules can enhance water uptake in the membrane and significantly improve the polymer chain mobility and CO_2 permeability (from 49.8 to 103 barrer) by strengthening the water swell effect. Incorporating *N*-isopropylacrylamide (NIPAM) hydrogel coated CNTs into Pebax 1657 can also improve the CO_2 separation performance of the pure polymer membrane. Similarly, the NIPAM hydrogel layer acts as the super water absorbent to increase the water content of membranes, enhancing CO_2 permeability and CO_2/gas selectivity simultaneously.[131]

Carboxymethyl chitosan (CMC) was used to modify the surface of TiO_2 nanoparticles in the fabrication of MMMs.[75] Strong interactions between C=O groups in Pebax 1657 with hydroxyl and amine groups in CMC are beneficial for reducing interfacial micro-gaps in MMMs. Besides, the amine groups facilitated the transport of CO_2 through reversible reactions. Therefore, both the CO_2 permeability and CO_2/N_2 selectivity are higher in the CMC–TiO_2/Pebax 1657 MMMs than in the pristine TiO_2/Pebax 1657 MMMs. Prasad and Mandal[132] blended a natural polymer, silk fibroin (SF), into graphene nanoparticles/chitosan MMMs. The inherent amines in SF contribute to the facilitated transport of CO_2. The introduction of other polymers with N-containing functional groups, such as poly(1-vinylimidazole)[133] and polyaniline,[134] into MMMs by filler modification also improved the CO_2 separation performance of the corresponding PMAA submicrocapsules/SPEEK and halloysite nanotubes/SPEEK MMMs.

Recently, a PI brush grafting modification strategy was applied by Li and co-workers to engineer the interface between the MOF filler and PI matrix.[135] The step-growth polymerization grafting process of PI is shown in Fig. 16(a). First, one end of the initial dianhydride monomers was anchored on the surface of UiO-66-NH_2 nanoparticles. Then, the other end of the anchored dianhydride monomers participated in the chain growth reaction to obtain a immobilized poly(amic acid) (PAA) layer on the particle surface. Finally, the PAA layer was turned into a PI brush layer through an imidization process. The PI brush grafted UiO-66-NH_2 nanoparticles have an excellent interparticle adhesion that can form a free-standing membrane even without the polymer matrix. In PI@UiO-66-NH_2/PI MMMs, the excellent compatibility between the compositionally identical PI brush and matrix leads to a more compact and integrated interfacial structure than that of the UiO-66-NH_2/PI MMMs, as demonstrated by Fig. 16(b). As a result, these MMMs exhibit significantly decreased interfacial tears (red circles), enhanced membrane breaking elongation (nearly 5 times that of the UiO-66-NH_2/PI membrane when the filler loading is 5 wt%), and improved CO_2 separation performance. A similar strategy has been adopted recently by Qian *et al.*[136] to improve the interfacial compatibility of UiO-66-NH_2/6FDA–durene MMMs. In this work, the PI oligomer with relatively low molecular weight was synthesized through controlled polymerization of monomers before being covalently attached to the surface of UiO-66-NH_2, instead of the *in situ* polymerization grafting process.

 This journal is © The Royal Society of Chemistry 2019

Published on 04 October 2019. Downloaded by Yunnan University on 8/23/2025 5:29:10 PM.

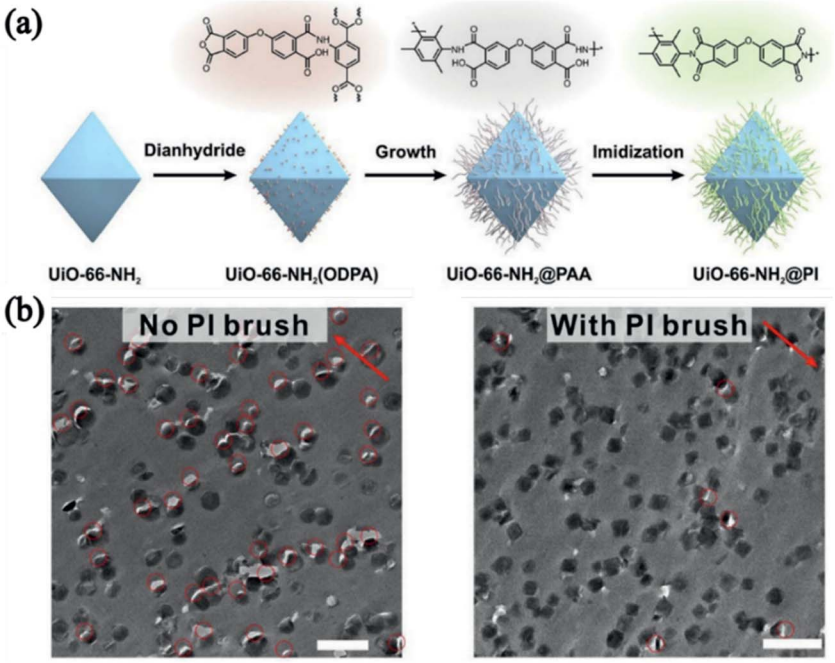

Fig. 16 (a) Synthetic procedures of PI brush grafted UiO-66-NH_2. (b) TEM images of ultrathin slices of MMMs containing 27 wt% pristine UiO-66-NH_2 and PI brushes grafted UiO-66-NH_2, scale bar 500 nm. The red arrows indicate the cutting direction and the red circles highlight the torn interface. Reproduced with permission from ref. 135. Copyright 2018, American Chemical Society.

With a similar idea in mind, Cao *et al.*[137] immobilized PVAm chains on the surface of a 2D COF filler before MMM fabrication, as shown in Fig. 17. The grafted PVAm chains have identical chemical composition to the polymer matrix and can blur the boundary between the COF filler and PVAm matrix to improve the filler–polymer interface compatibility. Moreover, it is observed that the PVAm matrix can be induced by the immobilized PVAm chains to penetrate into the oversized pore structure of the COF filler and adjust its pore size and chemical environment. Interestingly, the ideal selectivity of CO_2/N_2 in a MMM containing 10 wt% PVAm modified COF (COF_p) is very low (2.3), while the CO_2/N_2 mixed-gas selectivity is much higher (86). Possible explanations are as follows: (i) the pore size of the COF filler is much larger than the sizes of CO_2 and N_2 molecules, leading to a significantly decrease in diffusion selectivity of the MMM for CO_2 and N_2; (ii) the penetrated PVAm matrix can reduce the pore to a suitable size ($2d_{CO_2}$ < pore size < $2d_{CO_2}$ + d_{N_2}) and enhance CO_2 adsorption in the pores; and (iii) the preferential adsorption of CO_2 in the modified pore channels can crowd out N_2 molecules due to the suitable pore size and facilitate the competitive transport of CO_2 molecules. For the same reasons, the COF_p/PVAm MMM has a similar CO_2 permeance but a higher CO_2/N_2 selectivity compared with the original COF/PVAm MMM. These MMMs also exhibit good separation performance for CO_2/CH_4 and CO_2/H_2 gas mixtures.

Cohen and co-workers[138] covalently grafted the surface of UiO-66-allyl particles with hydride-terminated poly(-dimethylsiloxane) (PDMS) before embedding them into the PDMS matrix. The PDMS coating can improve the stability of MOF particles in toluene suspension by increasing the hydrophobicity, contributing to the excellent filler distribution in polymer matrix under a high filler loading (50 wt%). Besides,

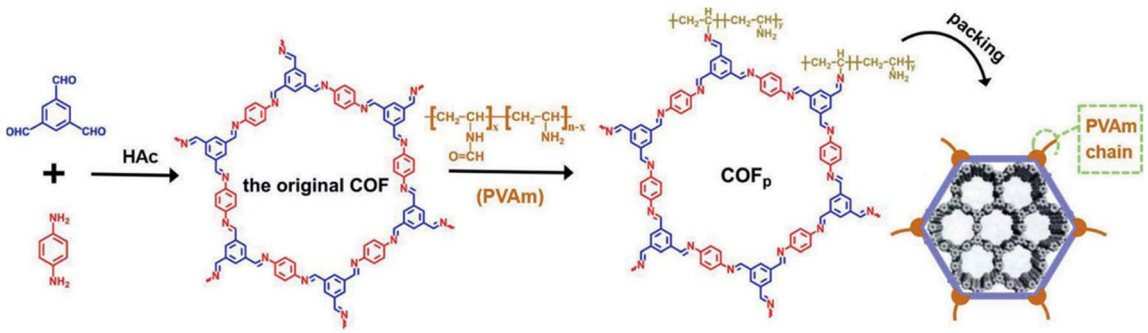

Fig. 17 Synthesis process and structure of COF_p. Reproduced with permission from ref. 137. Copyright 2019, American Chemical Society.

Published on 04 October 2019. Downloaded by Yunnan University on 8/23/2025 5:29:10 PM.

the PDMS-coating has identical chemical composition with the polymer matrix and the ability to participate in the crosslinking of the PDMS matrix, benefiting the formation of integrated interfacial morphology. Owing to these effects, high-loading defect-free MMMs with largely improved CO_2/N_2 separation performance could be successfully prepared. In contrast, the membrane containing 50 wt% original UiO-66-allyl particles experienced a significant loss in CO_2/N_2 separation performance due to the formation of non-selective voids.

As we can see, the abundant types and properties of macromolecules can offer rich possibilities for further improving the separation performance of MMMs. Besides the frequently studied PEG, PDA and PEI, it is anticipated that macromolecules having the same chemical composition or capable of cross-linking with the polymer matrix may have great potential in improving the filler–polymer interfacial structure of MMMs. However, there are only a few research studies in this area at present, which need to be strengthened in the future.

4 Porous materials as the third component

Recently, porous materials have been widely utilized as tertiary additives in MMM preparation. Besides helping improve the dispersion and compatibility of the original filler particles in/with the polymer matrix, the porous feature of this kind of third component may also introduce other effects, like providing additional gas transport channels, regulating gas transport paths, and enhancing molecular screening ability, in a synergistic manner with the original filler. Combining two kinds of fillers with different dimensions, pore structures, and chemical compositions may provide more opportunities for improving the structural peculiarity and separation performance of MMMs.

4.1 MOFs and COFs

Up to now, MOFs and COFs are the most frequently studied category of porous materials in ternary MMM fabrication. As a kind of novel porous functional materials, MOFs/COFs have attracted great attention during the past few decades.[139–142] The regular pore structure, adjustable pore size and chemical environment, advantages in the potential for modification, as well as the characteristic of containing polymer compatible organic components in the structure make them promising candidates as fillers in MMMs.[18,45,46,49,143] In fact, these materials can also be blended in some ternary MMMs as the secondary additive. For example, Coronas and co-workers[144] combined a MOF and zeolite in the same MMM for the first time in 2011, in which ZIF-8 or HKUST-1 was used to combine with silicalite-1. Among the prepared binary and ternary MMMs, the membrane containing an equal amount of HKUST-1 and silicalite-1 offers better CO_2/CH_4 and CO_2/N_2 selectivity than the counterparts, possibly due to the appropriate combination of the high CO_2 adsorption capacity of HKUST-1 and good compatibility of silicalite-1 with the PSF matrix. In their successive work,[145] replacing half of the filler in 16 wt% ZIF-8/PSF MMM with MIL-101(Cr) can enhance the diffusion selectivity of CO_2 due to the facilitated transport effect of coordinative unsaturated Cr sites in MIL-101(Cr) for CO_2, leading to an improved CO_2/CH_4 selectivity (from 22 to 40). They have also blended ZIF-8 (HKUST-1) nanoparticles into the IL-CS hybrid polymer matrix to improve the selectivity for CO_2/N_2 separation.[146] The selective pore channels of ZIF-8 and HKUST-1 with a low transport resistance for CO_2 molecules brought about simultaneously improved CO_2 permeability and CO_2/N_2 selectivity to the IL-CS membrane. The IL also contributed to the improvement in CO_2/N_2 selectivity by acting as a wetting medium between MOF particles and the CS matrix to reduce interfacial defects, reflecting the mutual influence between different components in the ternary system. The blending of ZIF-8 into $[emim][B(CN)_4]$,[147] *p*-nitro aniline,[148] GO,[149] PEG 200,[150] and piperazine glycinate (PG)[151] based MMMs as the third component has also been reported. In these MMMs, ZIF-8 mainly provided additional transport paths for gas molecules. Mahdavi and Moradi-Garakani[152] prepared a series of ternary MMMs by combining nonporous fumed silica and a novel trinuclear zinc MOF, $\{[Zn_3(tp)_4]\text{-}4H_2O\}_n$, in a PES matrix. The CO_2 permeability was greatly improved from 1.24 to 30.92 barrer due to the additional transport paths provided by the MOF. Meanwhile, the CO_2/CH_4 selectivity was also slightly enhanced.

Also, using the physical blending method, Sarfraz and Ba-Shammakh prepared a series of ternary MMMs containing MOFs and GO as fillers simultaneously.[153–155] ZIF-300, ZIF-301, and ZIF-302 used as the third component in these studies are mixed-linker ZIFs including 2-methylimidazole and different secondary imidazole linkers. These ZIFs can preferentially adsorb quadrupolar CO_2 molecules owing to their characteristic chemical and structural properties. Therefore, introducing these ZIFs can enhance the CO_2 solubility selectivity and diffusion coefficient of MMMs. In the meantime, the tortuous channels generated by horizontally arranged GO nanosheets can improve the diffusion selectivity of MMMs for CO_2. Synergetic effects between GO and the ZIF fillers at optimal loadings and proportion lead to a result that the CO_2 separation performance of these ternary MMMs is superior to that of the binary counterparts. For the CNTs/PSF MMMs, the introduction of well dispersed ZIF-302 (ref. 156) and ZIF-301 (ref. 157) nanoparticles can provide a significant steric effect to reduce CNT aggregation, thus exploiting the pore channels of CNTs to improve CO_2 permeability.

Samarasinghe *et al.*[158] combined a 2D MOF (CuBDC nanosheet) and a 3D MOF (ZIF-8) in one ODPA-TMPDA based MMM. In the binary MMM containing 10 wt% ZIF-8 alone, the CO_2 permeability increases from 112 barrer to 145 barrer compared with the neat ODPA-TMPDA membrane due to the additional transport channels provided by ZIF-8, while the CO_2/CH_4 selectivity remains unchanged. In the binary MMM containing only 2 wt% CuBDC nanosheets as the filler, the CO_2 permeability decreases from 112 barrer to 99 barrer, while the CO_2/CH_4 selectivity increases from 36 to 43 benefiting from the enhanced diffusion selectivity of CO_2. Both ZIF-8 and CuBDC nanosheets have shown some shortcomings in improving the CO_2 separation performance of polymer membranes. In

 This journal is © The Royal Society of Chemistry 2019

Published on 04 October 2019. Downloaded by Yunnan University on 8/23/2025 5:29:10 PM.

comparison, the ternary MMM containing 10 wt% ZIF-8 and 2 wt% CuBDC nanosheets shows a better CO_2/CH_4 separation performance by combining the advantages of the two kinds of MOFs.

The mixed filler strategy has also been adopted in other application scenarios. For example, the combination of mesoporous MCM-41 with microporous layered titanosilicate (JDF-L1, with a pore size of about 0.3 nm) in 6FDA-4MPD/6FDA-DABA copolyimide can achieve proper balance between improving H_2 permeability and H_2/CH_4 selectivity, compared to the binary counterparts containing merely MCM-41 or JDF-L1.[159] The JDF-L1 sheets with a preferential horizontal orientation provide increase in H_2 selectivity while improving the dispersion of MCM-41 particles in the MMMs, and the mesoporous MCM-41 provides fast transport channels for gas molecules. Similarly, the combination of MCM-41 with NH_2-MIL-53(Al) in PSF can also achieve an improvement in H_2/CH_4 separation by integrating the interesting characteristics of two different fillers.[160]

In comparison to the direct physical blending method, it is demonstrated that constructing a core@shell structural composite is an effective way to integrate the interesting properties of two different components including MOFs in MMMs. For example, Sorribas *et al.*[161] prepared a silica@ZIF-8 core@shell filler *via in situ* growth for MMM fabrication. Although they did not compare with the silica/PSF MMMs, the maintained CO_2/CH_4 selectivity of the silica@ZIF-8/PSF MMMs at filler loadings up to 32 wt% suggests that the composite filler has good compatibility with the polymer matrix mainly benefitting from the ZIF-8 shell, which is quite rare when using pure inorganic fillers like silica. Lin *et al.*[162] decorated a NH_2-MIL-101(Al) shell on the surface of carboxyl-modified CNTs and further applied the CNT@MOF filler in MMM fabrication. The extra amine groups and active sites introduced by NH_2-MIL-101(Al) can increase the CO_2 adsorption capacity and selectivity of the membrane, while the CNTs provide fast transport channels for gas molecules. The 5 wt% NH_2-MIL-101(Al)@CNT/6FDA–durene MMM exhibits significantly improved CO_2/CH_4 selectivity compared with the CNT-based MMM with the same filler loading, while maintaining high permeability.

Song *et al.*[163] *in situ* grew a ZIF-8 layer on the surface of UiO-66-NH_2 particles *via* a layer-by-layer method and further incorporated the obtained core@shell material into the PSF matrix. As shown in Fig. 18, the ZIF-8@UiO-66-NH_2/PSF membrane exhibits a largely improved CO_2/N_2 selectivity (from 25 to 39) compared with the control membrane containing 40 wt% pristine UiO-66-NH_2. The increase in CO_2/N_2 selectivity may be benefitted from the enhanced molecular sieving effect for CO_2 and N_2 due to the small pores of the ZIF-8 shell and even smaller pores generated at the interface by the imperfect registry between the overlapping pores of ZIF-8 and UiO-66-NH_2. Moreover, no obvious sacrifice in CO_2 permeability was observed, indicating that the large pore channels of UiO-66-NH_2, for ensuring fast gas transport, can be preserved in the composite and the ultra-thin ZIF-8 layer did not increase the mass transfer resistance significantly.

Sánchez-Laínez *et al.*[164] prepared a ZIF-8@ZIF-7 core@shell composite through a post-synthetic linker exchange modification method. The composite filler has better compatibility with the polybenzimidazole (PBI) matrix than the pristine ZIF-8 filler because of the benzimidazole ligand from ZIF-7 in the shell layer. Moreover, since ZIF-7 has a smaller pore window than ZIF-8, the conversion of the surface of ZIF-8 into ZIF-7 can also enhance its sieving effect to H_2 and CO_2 molecules. Due to the above reasons, the 20 wt% ZIF-8@ZIF-7/PBI MMM exhibits a better separation performance for the H_2/CO_2 mixture than the ZIF-8/PBI MMM with the same filler loading. By immersing ZIF-93 in the solution of the benzimidazole linker, they also prepared a ZIF-93@ZIF-11 core@shell composite. The ZIF-11 layer on the surface of ZIF-93 can also improve its compatibility with the PBI matrix and constrain its microporosity, leading to an enhancement in the H_2/CO_2 separation factor.[165]

Because of their organic nature, COFs are generally considered to have better compatibility with organic polymers than inorganic fillers, even MOFs. For this reason, Cheng *et al.*[166] synthesized a UiO-66-NH_2@TpPa-1 core@shell filler through a sequential process composed of surface functionalization and *in situ* polymerization on the UiO-66-NH_2 particle surface, as shown in Fig. 19. Embedding this composite into PSF can generate a well-integrated and defect-less interface between the

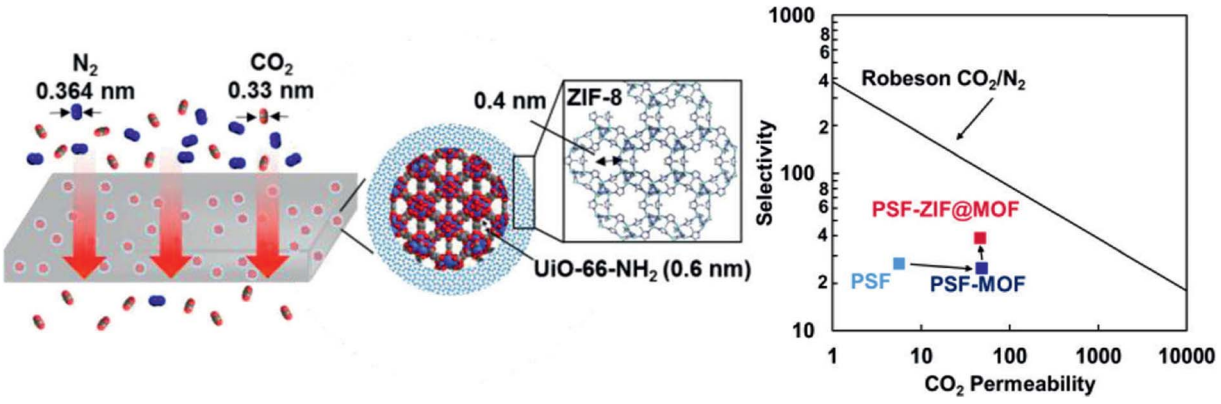

Fig. 18 Schematic structures of the MMMs and UiO-66-NH_2@ZIF-8 core@shell filler, and the CO_2/N_2 separation performance of the UiO-66-NH_2@ZIF-8/PSF MMMs. Reproduced with permission from ref. 163. Copyright 2017, American Chemical Society.

Published on 04 October 2019. Downloaded by Yunnan University on 8/23/2025 5:29:10 PM.

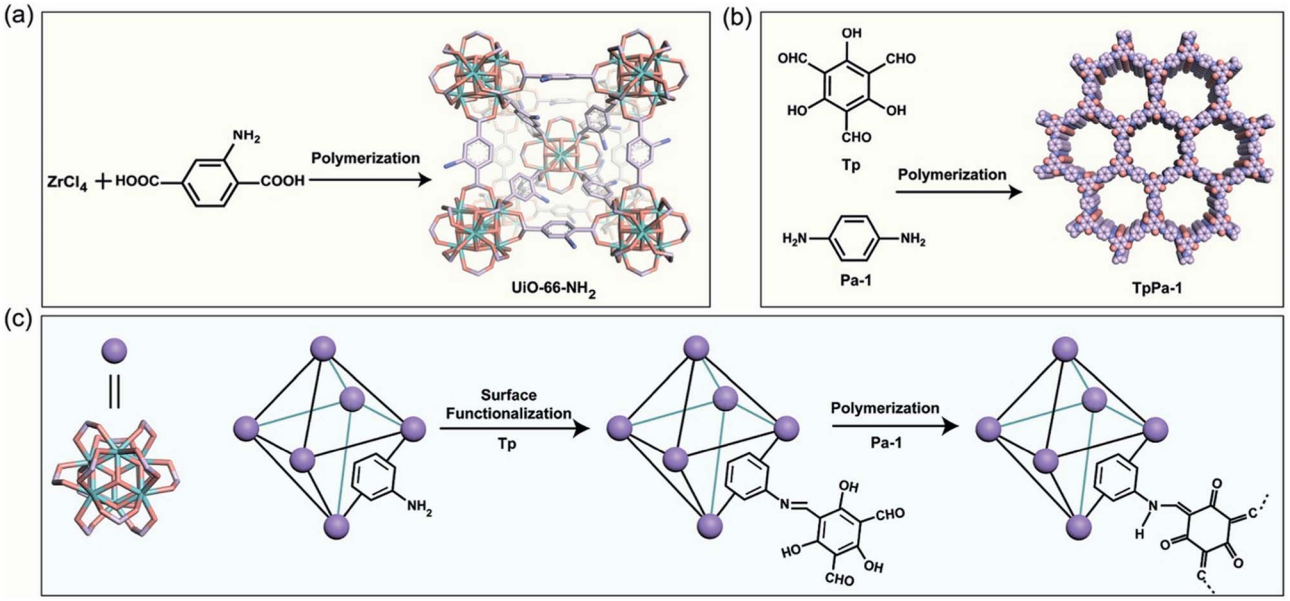

Fig. 19 Preparation of (a) MOF UiO-66-NH_2, (b) COF TpPa-1, (c) MOF@COF hybrid material. Reproduced with permission from ref. 166. Copyright 2019, Elsevier B.V.

filler and polymer matrix due to the improved interfacial compatibility. As a result, the UiO-66-NH_2@TpPa-1/PSF MMM containing 5 wt% filler loading exhibits an apparent increase in CO_2/CH_4 selectivity (from 26.1 to 46.7) compared with the neat PSF membrane when the corresponding UiO-66-NH_2/PSF is experiencing a decrease (from 26.1 to 22.1).

GO laminates have been frequently used as the filler in MMM fabrication. Because of the large aspect ratio and small interlayer spacing, GO laminates prefer to distribute in MMMs parallel to the membrane surface and significantly change the transport paths of gas molecules to more tortuous and discriminative ones. Besides, the abundant CO_2-philic oxygen-containing functional groups in GO laminates can accelerate the preferential adsorption and transport of CO_2. Therefore, incorporating GO laminates usually can significantly improve the diffusion selectivity of membranes for CO_2 towards larger gas molecules, for example CH_4 and N_2. However, the diffusion coefficient of membranes is often negatively affected, resulting in decreases in gas permeability. Moreover, the improvement in the gas separation performance is always limited by improving the diffusion selectivity alone. To address these problems, some researchers introduced MOFs into GO-based MMMs by *in situ* growth of MOF particles on the surface of the GO lamellar filler.[167–172] With the aid of the good diffusion or/and adsorption properties of MOFs, the separation performance of the original GO-based MMMs could be readily improved.

For example, Dong *et al.*[167] prepared a ZIF-8@GO composite *via* an *in situ* growth method for MMM fabrication. The carboxyl groups on GO nanosheets can anchor Zn ions and provide nucleation and growth sites for ZIF-8 crystals. Two-component GO/Pebax 2533 and ZIF-8/Pebax 2533 MMMs were also prepared for comparison. As usual, the incorporation of GO nanosheets

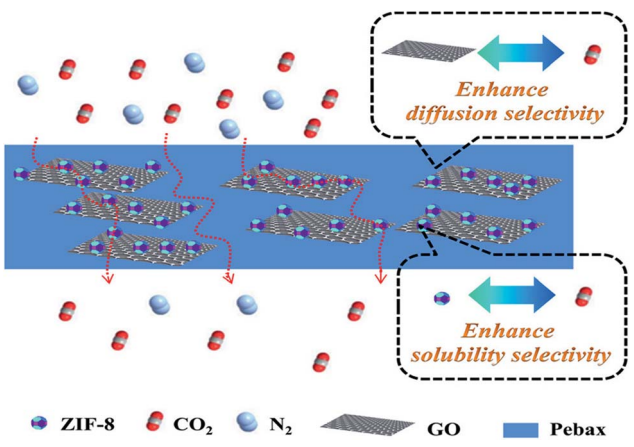

Fig. 20 Schematic illustration of the transport mechanism for the ZIF-8@GO/Pebax 2533 MMMs. Reproduced with permission from ref. 167. Copyright 2016, Elsevier B.V.

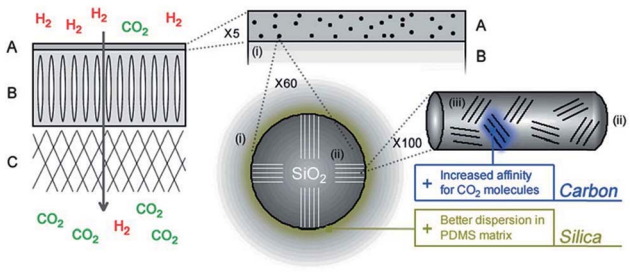

Fig. 21 Schematic of the membrane structure. (A) Dense PDMS top layer containing porous CSM fillers (i), of which the mesopores (ii) are filled with functionalised carbon (iii); (B) asymmetric porous PI support layer; (C) polypropylene nonwoven layer. Reproduced with permission from ref. 174. Copyright 2013, Royal Society of Chemistry.

This journal is © The Royal Society of Chemistry 2019

Published on 04 October 2019. Downloaded by Yunnan University on 8/23/2025 5:29:10 PM.

Table 1 Summary of the different roles and functionalities observed for the third components

	Roles and functionalities	Strategy	The third components	Key properties of the third components
1	Eliminating interfacial voids	Filling-in the gap	ILs,[58–63,72] liquid sulfolane,[87] PEG 200 (ref. 96)	Existing in the liquid form; good wettability for both the filler and polymer matrix
		Binding the border	ILs,[65,67–71] organic silanes,[73–76] HMA,[86] norbornene,[94] EDA,[92] PEGs,[92,99,101,103,104] CMC,[75] PDA,[109,110] PEI,[114–116,119,122,127,128] PDMS,[138] SiO_2 (ref. 177)	Reactive or/and have strong interactions with both the filler and polymer
			Phenyl acetyl,[93] polyimide,[135,136] PVAm,[137] PDMS,[138] ZIFs,[161,164,165,173] TpPa-1 (ref. 156)	Reactive with the filler and containing a similar chemical composition to the polymer
2	Reducing the effective pore size	Cavity-occupying	ILs,[64,65] Co^{2+}–diamine–diketone complex[91]	Appropriate molecular volume
		Suppressing linker distortion	EDA[89]	Covalent coupling linker and polymer matrix
		Surface pore overlapping	ZIF-8,[161] ZIF-7,[162] ZIF-11 (ref. 163)	With smaller pore size than the existing filler
3	Improving filler distribution	Stabilizing the filler suspension *via* decreasing the surface free energy	PEGs,[99,103] PEI,[126] PVP[129]	Large contact area with surrounding substances
		Changing the polarity or/and hydrophilicity/ hydrophobicity of the filler surface	APTMS,[73] GTA[90]	Similar polarity and hydrophilicity/ hydrophobicity to the solvent for membrane fabrication
		Inhibiting aggregate formation by the steric effect	ZIFs,[153–157,167,168,170,172,173] UiO-66,[169] UiO-66-NH_2,[171] CNT,[176] halloysite nanotubes[177]	Different dimensions from the existing filler
4	Increasing CO_2 diffusion selectivity	Facilitating CO_2 transport	NH_2-IL,[66] APTES,[73,77] metal ions,[78,79,82–84] Co^{2+}–diamine–diketone complex,[91] EDA,[92] PEI,[102,114–116,119,122,126] PDA,[110] other N-containing polymers[130–134]	Reversible reaction with CO_2 molecules
		Hindering the diffusion of competitive molecules	ILs,[64–66] PEGMA,[103] ZIF-8,[163] ZIF-7,[164] ZIF-11 (ref. 165)	Ability to reduce the effective pore size
			ZIF-8,[146] HKUST-1,[146] SAPO-34 (ref. 180)	Suitable pore aperture for screening CO_2 and larger molecules
			CuBDC nanosheets,[158] GO[176–178]	Ability to form tortuous and discriminative transport paths
5	Increasing CO_2 solubility selectivity	Enhancing CO_2 adsorption	IL,[60,61,63–66,68–70] organic silanes,[73,75] metal ions,[80,81,85] DEA,[88] EDA,[92] PEGs,[92,96–103] PEI,[102,114–116,119,122,126–128] chitosan,[75] MOFs,[144–146,152–157,162,171] carbon[174,175]	Containing CO_2-philic functional groups
6	Reducing pore blockage	Detaching polymer chains from the surface of filler particles	APDEMS,[33] 4-cyanobenzoyl chloride[95]	Reactive with the filler surface
7	Controlling filler orientation	Bridging the filler with a directing agent	APTES[74]	Reactive with the filler and directing agent

Published on 04 October 2019. Downloaded by Yunnan University on 8/23/2025 5:29:10 PM.

Table 1 (*Contd.*)

	Roles and functionalities	Strategy	The third components	Key properties of the third components
8	Providing additional transport paths	Introducing porous materials as the third component	MOFs,[146–157,167–173] CNTs,[176] halloysite nanotubes,[177] SAPO-34 (ref. 180)	Porosity
9	Improving mechanical properties	Binding the border of the filler and polymer matrix	IL,[65] norbornene,[94] PDA,[109] PEI,[126] polyimide,[135,136] PDMS[138]	Reactive or/and have strong interactions with both the filler and polymer
10	Increasing the fractional free volume	Plasticizing the polymer matrix	IL,[62] PEGs,[98] GTA[90]	Ability to decrease interactions between polymer chains
		Disrupting polymer chain packing	GO,[176–178] CuBDC nanosheets[158]	Large radial dimension
11	Stiffening the polymer matrix	Increasing interactions between polymer chains	HMA,[86] EDA[89]	Strong interaction with polymer chains

alone brings about an increase in CO_2/N_2 (from 27 to 31), but a decrease in CO_2 permeability (from 132 to 120 barrer). The incorporation of ZIF-8 alone improved the CO_2 permeability and CO_2/N_2 selectivity from 132 to 180 barrer and 27 to 35, respectively, because of the CO_2 adsorption selectivity and extra transport channels provided by ZIF-8. Among the three kinds of MMMs with the same filler loading, the 6 wt% ZIF-8@GO/Pebax 2533 MMM exhibits the largest improvement in both CO_2 permeability (from 132 to 249 barrer) and CO_2/N_2 selectivity (from 27 to 47.6). The schematic illustration of the transport mechanism for the ZIF-8@GO/Pebax 2533 MMMs is shown in Fig. 20. The large improvement in CO_2/N_2 selectivity can be attributed to the simultaneous enhancement in CO_2 diffusion selectivity and solubility selectivity due to GO and ZIF-8 respectively. For the improvement in CO_2 permeability, the combined effects of the fast diffusion in ZIF-8 channels, facilitated transport by the polar functional groups from the GO nanosheets, disrupted arrangement of polymer chain packing, and the large free volume introduced by ZIF-8@GO should be responsible. For a similar purpose, Zhang *et al.*[173] prepared a heterostructured filler by *in situ* growth of ZIF-8 on the surface of layered double hydroxide (LDH) nanosheets. The ZnAl–CO_3 LDH can provide the Zn source for ZIF-8 crystallization. Interfacial compatibility between the LDH and the Pebax 1657 matrix is improved by the ZIF-8 layer. Moreover, the presence of ZIF-8 can increase the CO_2 concentration around the LDH due to preferential adsorption of CO_2, thus accelerating the CO_2 facilitated transport effect of LDHs.

4.2 Carbon materials

Vankelecom and coworkers[174] prepared a carbon-silica material (CSM) through *in situ* polymerization and pyrolysis of carbon precursors (furfuryl alcohol and mesitylene) in the pores of MCM-41. Incorporating this CSM filler into a thin selective PDMS layer of the PDMS/PI composite membrane can result in an improvement in CO_2/H_2 selectivity (from 2.4 to 6.0 at 30 wt% filler loading), as shown in Fig. 21. The increase can be attributed to the enhanced CO_2 adsorption in the filler because of the interactions between the quadrupolar CO_2 molecules and oxygen-containing functional groups provided by the introduced carbon component. Applying this kind of CSM as the filler in Matrimid® 9725 can also improve the CO_2/CH_4 and CO_2/N_2 selectivity while maintaining the CO_2 permeability due to the enhancement in solubility selectivity of the membrane.[175]

Li *et al.*[176] prepared ternary MMMs by blending CNTs and GO. The total amount of filler in the Matrimid® 5218 matrix was fixed at 10 wt%. An optimal CO_2 separation performance, better than that of the MMMs incorporated with either CNTs or GO alone, was achieved using an equal amount of CNTs and GO, suggesting that there is a favourable synergistic effect between CNTs and GO. In the MMMs containing only CNTs, the CNTs were designed to enhance the permeability of the membrane because of their large and smooth pore channels. However, according to the characterization results, they tended to agglomerate at high loading (10 wt%), limiting the full exploitation of their properties with only a slight improvement in CO_2 permeability (from 8.84 to 10.29 barrer). In contrast, the CNTs and GO nanosheets can be well dispersed with a preferential horizontal orientation in the optimal ternary MMM. The CNTs can reduce the re-stacking of GO nanosheets and provide fast transport channels for preferentially adsorbing CO_2 molecules and thus greatly improve the CO_2 permeability and selectivity simultaneously.

Dong *et al.*[177] prepared a series of dual-inorganic composite membranes by assembling porous reduced GO and halloysite nanotubes, two different fillers with a largely different aspect-ratio, into the Pebax 1657 matrix. Considering the porous reduced GO as the third component, its addition can greatly enhance the diffusion selectivity of CO_2 in MMMs due to the associated tortuous and discriminative transport path. Therefore, the MMM containing 0.15 wt% halloysite nanotubes and 0.02 wt% porous reduced GO exhibits a significant improvement in CO_2/N_2 selectivity compared with the 0.15 wt% halloysite nanotubes/Pebax 1657 MMM (from 42 to 118). A similar effect of GO on improving CO_2 diffusion selectivity was also

 This journal is © The Royal Society of Chemistry 2019

Published on 04 October 2019. Downloaded by Yunnan University on 8/23/2025 5:29:10 PM.

discovered in the poly(ethylene glycol) methyl ethyl acrylate (PEG-MEA)/GO/Pebax 1657 MMMs.[178]

4.3 Other materials

Zeolites, silica, and other porous materials have also been introduced into MMMs as the secondary filler to enhance the CO_2 separation performance. For example, in the halloysite nanotubes/porous reduced GO/Pebax 1657 MMMs,[177] the halloysite nanotubes can be considered as the supplementary filler for porous reduced GO/Pebax 1657 MMMs. Their introduction was designed to increase the diffusion coefficient of the membrane by providing fast transport channels for gas molecules, and the role is confirmed by the increase in CO_2 permeability of the 0.02 wt% porous reduced GO/Pebax 1657 MMM. Interestingly, the CO_2/N_2 selectivity is also improved from 78 to 118, suggesting that there exists a synergistic effect between halloysite nanotubes and porous reduced GO nanosheets on the optimization of transport pathways for gas molecules. Hou *et al.*[179] found that coating MWCNTs with a mesoporous SiO_2 layer can improve the filler–polymer interfacial compatibility in SiO_2@MWCNTs/Pebax 1657 MMMs to some extent, leading to higher CO_2/CH_4 and CO_2/N_2 selectivity at a relative high filler loading (10 wt%) than the 10 wt% MWCNTs/Pebax 1657 MMM because of the elimination of interfacial voids. In the SAPO-34/[emim][TF_2N]/poly(IL) MMMs, SAPO-34 can enhance the CO_2 diffusion and solubility selectivity of the membrane, thus improving the CO_2 permeability and CO_2/CH_4 selectivity simultaneously.[180]

5 Conclusion and outlook

With the development of the membrane separation technology, the increasing demand for high-performance membranes led to extensive research on MMMs. During the past few decades, many kinds of materials have been used as fillers in the fabrication of MMMs. Besides developing new fillers with advanced properties, the introduction of various kinds of tertiary components can also significantly improve the separation performance, opening a novel avenue for producing MMMs with unique structures and outstanding performance. In the past few years, various materials, including ILs, organic small molecules, macromolecules, and MOFs/COFs, have been introduced into MMMs as the third component through physical blending, filler modification, and post-treatment of the membrane, inducing significantly improved separation performance of the original MMMs, especially in CO_2 capture.

In general, the merits of ternary MMMs are related to the plenty of opportunities in optimizing the membrane morphology and separation performance brought about by the various functionalities of the third component, which are summarized in Table 1, together with the design strategies, the third component providing the functionalities, and the key properties of these third components. Small molecules, macromolecules and porous materials exhibit special advantages in different aspects due to their different intrinsic properties, for example porous materials in providing additional transport paths. Choosing the appropriate third component according to the actual needs is the key to obtain high performance ternary MMMs.

Since the non-idealities in membrane morphology, especially the interfacial voids due to incompatibility between the filler and polymer, have been commonly considered as the most important problem in MMM fabrication, we take the elimination of non-selective voids as the most desired effect for a third component among the proposed functionalities. In this respect, materials having the ability to crosslink the filler and polymer or those with identical (similar) chemical compositions to the polymer matrix may be efficient tertiary components for MMM fabrication. With the aid of the third components, ternary MMMs may play an important role in the development of high flux ultrathin MMMs for industrial application, since ultrathin MMMs have much lower tolerance to particle agglomeration and filler–polymer interfacial defects than thick MMMs. From the perspective of industrial application, the third components that can improve the repeatability and stability in membrane fabrication are also highly demanded.

Although great progress has been achieved, there is still room for improving the development of multicomponent MMMs in the future. First, it is urgent to develop a high-throughput screening method of the third component for MMMs. As known, there is already a huge and growing material library for traditional fillers. The introduction of the third component and its matching with the original filler will expand the material library to a tremendous extent. For example, countless composite materials can be produced just by the combination of ILs and MOFs. It is impossible to study the effects of these tremendous combinations on MMMs solely by experiment. In this regard, the materials genomics method[181–183] may be an effective tool. In our recent work,[184] 550 357 IL@MOF composites were computational assembled and screened for CO_2 capture, which is a typical example for the application of the materials genomics method in large-scale material screening.

Second, the microstructural characterization of ternary MMMs should be performed using advanced equipment and techniques for the study of the separation mechanism. For example, synergistic effects between two different fillers with a largely different aspect-ratio have been discovered in many MMMs. However, clear characterization results of the distribution of two different materials in the membrane have hardly been obtained, leaving the mechanism analysis on the synergistic effects between fillers and changes of separation performance remaining at the conjecture stage. In this respect, for example, TEM characterization of ultrathin slices of the membrane cross section applied in the work of Wang *et al.*[135] and tomographic focused ion beam scanning electron microscopy (FIB-SEM) characterization applied by Gascon and coworkers[185,186] may provide guidance. The development of new and non-destructive characterization methods for the membrane microstructure is also highly encouraged.

Third, investigation of the factors influencing the filler–polymer interfacial structure is needed. The introduction of the third component has been proven to be able to improve the

Published on 04 October 2019. Downloaded by Yunnan University on 8/23/2025 5:29:10 PM.

interfacial structure in many MMMs. However, there still lacks general rules on how to design the interface structure. A combination of computational and experimental methods in studying the filler–polymer interfacial interactions may help promote better understanding that can guide the design of new MMMs with improved properties.

Fourth, the unpredictable filler distribution and filler–polymer interfacial morphology make it very difficult to understand the transport mechanism of MMMs, making it infeasible to predict and optimize the performance of the MMM module with computational fluid-dynamic (CFD) modelling. Although in some cases the introduction of the third component can simplify the structure of MMMs to more ideal ones, in most times, more complicated structures and compositions will be obtained. Modifying the fluid-dynamic models to describe the mass transfer mechanism of ternary MMMs more accurately is needed in the future.

With the development in the aforementioned aspects, particularly a combinational study of computation and experiment, MMMs with excellent CO_2 separation performance can be realized. In addition, combining the abundant functionalities of these fillers, for example the catalytic activity, reactive separation may be an exciting field which deserves more attention. More importantly, the advantages of ternary MMMs in optimizing the membrane structure and separation performance, improving repeatability and stability in membrane fabrication, providing opportunities for preparing high flux ultrathin MMMs, and enhancing mechanical strength compared with binary MMMs make them promising candidates for other industrial applications, not limited to the CO_2 separation discussed in this review.

Conflicts of interest

There are no conflicts to declare.

Acknowledgements

This work was supported by the National Natural Science Foundation of China (Grant Numbers 21536001, 21878229 and 21606007) and the Science and Technology Plans of Tianjin (No. 18PTSYJC00180).

References

1 N. Du, H. B. Park, M. M. Dal-Cin and M. D. Guiver, *Energy Environ. Sci.*, 2012, **5**, 7306–7322.
2 C. A. Scholes, G. W. Stevens and S. E. Kentish, *Fuel*, 2012, **96**, 15–28.
3 T. C. Merkel, M. Zhou and R. W. Baker, *J. Membr. Sci.*, 2012, **389**, 441–450.
4 H. Yang, Z. Xu, M. Fan, R. Gupta, R. B. Slimane, A. E. Bland and I. Wright, *J. Environ. Sci.*, 2008, **20**, 14–27.
5 P. Bernardo, E. Drioli and G. Golemme, *Ind. Eng. Chem. Res.*, 2009, **48**, 4638–4663.
6 A. Brunetti, F. Scura, G. Barbieri and E. Drioli, *J. Membr. Sci.*, 2010, **359**, 115–125.
7 M. K. Mondal, H. K. Balsora and P. Varshney, *Energy*, 2012, **46**, 431–441.
8 Y. Zhang, J. Sunarso, S. Liu and R. Wang, *Int. J. Greenhouse Gas Control*, 2013, **12**, 84–107.
9 T.-S. Chung, L. Y. Jiang, Y. Li and S. Kulprathipanja, *Prog. Polym. Sci.*, 2007, **32**, 483–507.
10 M. Rezakazemi, A. E. Amooghin, M. M. Montazer-Rahmati, A. F. Ismail and T. Matsuura, *Prog. Polym. Sci.*, 2014, **39**, 817–861.
11 B. Seoane, J. Coronas, I. Gascon, M. E. Benavides, O. Karvan, J. Caro, F. Kapteijn and J. Gascon, *Chem. Soc. Rev.*, 2015, **44**, 2421–2454.
12 Y. Cheng, Z. Wang and D. Zhao, *Ind. Eng. Chem. Res.*, 2018, **57**, 4139–4169.
13 M. A. Aroon, A. F. Ismail, T. Matsuura and M. M. Montazer-Rahmati, *Sep. Purif. Technol.*, 2010, **75**, 229–242.
14 J. Dechnik, J. Gascon, C. J. Doonan, C. Janiak and C. J. Sumby, *Angew. Chem., Int. Ed.*, 2017, **56**, 9292–9310.
15 M. Galizia, W. S. Chi, Z. P. Smith, T. C. Merkel, R. W. Baker and B. D. Freeman, *Macromolecules*, 2017, **50**, 7809–7843.
16 L. M. Robeson, *J. Membr. Sci.*, 1991, **62**, 165–185.
17 L. M. Robeson, *J. Membr. Sci.*, 2008, **320**, 390–400.
18 W. Li, Y. Zhang, Q. Li and G. Zhang, *Chem. Eng. Sci.*, 2015, **135**, 232–257.
19 S. R. Venna and M. A. Carreon, *Chem. Eng. Sci.*, 2015, **124**, 3–19.
20 Y. Liu, Y. Ban and W. Yang, *Adv. Mater.*, 2017, **29**, 1606949.
21 Y. Shen and A. C. Lua, *Chem. Eng. J.*, 2012, **188**, 199–209.
22 S. Kim, E. Marand, J. Ida and V. V. Guliants, *Chem. Mater.*, 2006, **18**, 1149–1155.
23 B. D. Reid, F. A. Ruiz-Trevino, I. H. Musselman, K. J. Balkus and J. P. Ferraris, *Chem. Mater.*, 2001, **13**, 2366–2373.
24 O. G. Nik, X. Y. Chen and S. Kaliaguine, *J. Membr. Sci.*, 2012, **413–414**, 48–61.
25 R. Lin, B. V. Hernandez, L. Ge and Z. Zhu, *J. Mater. Chem. A*, 2018, **6**, 293–312.
26 V. C. Souza and M. G. N. Quadri, *Braz. J. Chem. Eng.*, 2013, **30**, 683–700.
27 N. Jusoh, Y. F. Yeong, T. L. Chew, K. K. Lau and A. M. Shariff, *Sep. Purif. Rev.*, 2016, **45**, 321–344.
28 R. Lin, L. Ge, L. Hou, E. Strounina, V. Rudolph and Z. Zhu, *ACS Appl. Mater. Interfaces*, 2014, **6**, 5609–5618.
29 T. Yang, Y. Xiao and T.-S. Chung, *Energy Environ. Sci.*, 2011, **4**, 4171–4180.
30 T.-H. Bae, J. S. Lee, W. Qiu, W. J. Koros, C. W. Jones and S. Nair, *Angew. Chem., Int. Ed.*, 2010, **49**, 9863–9866.
31 D. Bastani, N. Esmaeili and M. Asadollahi, *J. Ind. Eng. Chem.*, 2013, **19**, 375–393.
32 Y. Li, T.-S. Chung, C. Cao and S. Kulprathipanja, *J. Membr. Sci.*, 2005, **260**, 45–55.
33 Y. Li, H. M. Guan, T.-S. Chung and S. Kulprathipanja, *J. Membr. Sci.*, 2006, **275**, 17–28.
34 T. C. Merkel, B. D. Freeman, R. J. Spontak, Z. He, I. Pinnau, P. Meakin and A. J. Hill, *Chem. Mater.*, 2003, **15**, 109–123.
35 G. Clarizia, C. Algieri and E. Drioli, *Polymer*, 2004, **45**, 5671–5681.

 This journal is © The Royal Society of Chemistry 2019

Published on 04 October 2019. Downloaded by Yunnan University on 8/23/2025 5:29:10 PM.

36 M. Moaddeb and W. J. Koros, *J. Membr. Sci.*, 1997, **125**, 143–163.
37 B. Zornoza, S. Irusta, C. Téllez and J. Coronas, *Langmuir*, 2009, **25**, 5903–5909.
38 B. Zornoza, C. Téllez and J. Coronas, *J. Membr. Sci.*, 2011, **368**, 100–109.
39 B. Zornoza, C. Téllez, J. Coronas, O. Esekhile and W. J. Koros, *AIChE J.*, 2015, **61**, 4481–4490.
40 L. Ge, W. Zhou, V. Rudolph and Z. Zhu, *J. Mater. Chem. A*, 2013, **1**, 6350–6358.
41 A. Sabetghadam, B. Seoane, D. Keskin, N. Duim, T. Rodenas, S. Shahid, S. Sorribas, C. L. Guillouzer, G. Clet, C. Tellez, M. Daturi, J. Coronas, F. Kapteijn and J. Gascon, *Adv. Funct. Mater.*, 2016, **26**, 3154–3163.
42 B. Seoane, V. Sebastián, C. Téllez and J. Coronas, *CrystEngComm*, 2013, **15**, 9483–9490.
43 L. Diestel, N. Wang, B. Schwiedland, F. Steinbach, U. Giese and J. Caro, *J. Membr. Sci.*, 2015, **492**, 181–186.
44 N. Tien-Binh, D. Rodrigue and S. Kaliaguine, *J. Membr. Sci.*, 2018, **548**, 429–438.
45 H. B. T. Jeazet, C. Staudt and C. Janiak, *Dalton Trans.*, 2012, **41**, 14003–14027.
46 I. Erucar, G. Yilmaz and S. Keskin, *Chem.–Asian J.*, 2013, **8**, 1692–1704.
47 R. Nasir, H. Mukhtar, Z. Man and D. F. Mohshim, *Chem. Eng. Technol.*, 2013, **36**, 717–727.
48 G. Dong, H. Lia and V. Chen, *J. Mater. Chem. A*, 2013, **1**, 4610–4630.
49 B. Zornoza, C. Tellez, J. Coronas, J. Gascon and F. Kapteijn, *Microporous Mesoporous Mater.*, 2013, **166**, 67–78.
50 E. V. Perez, C. Karunaweera, I. H. Musselman, K. J. Balkus Jr and J. P. Ferraris, *Processes*, 2016, **4**, 32.
51 M. Wang, Z. Wang, S. Zhao, J. Wang and S. Wang, *Chin. J. Chem. Eng.*, 2017, **25**, 1581–1597.
52 M. Vinoba, M. Bhagiyalakshmi, Y. Alqaheem, A. A. Alomair, A. Pérez and M. S. Rana, *Sep. Purif. Technol.*, 2017, **188**, 431–450.
53 J. Dechnik, C. J. Sumby and C. Janiak, *Cryst. Growth Des.*, 2017, **17**, 4467–4488.
54 Y. Cheng, Y. Ying, S. Japip, S.-D. Jiang, T.-S. Chung, S. Zhang and D. Zhao, *Adv. Mater.*, 2018, **30**, 1802401.
55 M. Ramdin, T. W. de Loos and T. J. H. Vlugt, *Ind. Eng. Chem. Res.*, 2012, **51**, 8149–8177.
56 J. E. Bara, D. E. Camper, D. L. Gin and R. D. Noble, *Acc. Chem. Res.*, 2010, **43**, 152–159.
57 Y. Chen, Z. Hu, K. M. Gupta and J. Jiang, *J. Phys. Chem. C*, 2011, **115**, 21736–21742.
58 Y. C. Hudiono, T. K. Carlisle, J. E. Bara, Y. Zhang, D. L. Gin and R. D. Noble, *J. Membr. Sci.*, 2010, **350**, 117–123.
59 R. Shindo, M. Kishida, H. Sawa, T. Kidesaki, S. Sato, S. Kanehashi and K. Nagai, *J. Membr. Sci.*, 2014, **454**, 330–338.
60 C. Casado-Coterillo, M. D. M. López-Guerrero and Á. Irabien, *Membranes*, 2014, **4**, 287–301.
61 D. F. Mohshim, H. Mukhtar and Z. Man, *Sep. Purif. Technol.*, 2014, **135**, 252–258.
62 M. Li, X. Zhang, S. Zeng, L. bai, H. Gao, J. Deng, Q. Yang and S. Zhang, *RSC Adv.*, 2017, **7**, 6422–6431.
63 E. G. Estahbanati, M. Omidkhah and A. E. Amooghin, *ACS Appl. Mater. Interfaces*, 2017, **9**, 10094–10105.
64 Y. Ban, Z. Li, Y. Li, Y. Peng, H. Jin, W. Jiao, A. Guo, P. Wang, Q. Yang, C. Zhong and W. Yang, *Angew. Chem., Int. Ed.*, 2015, **54**, 15483–15487.
65 H. Li, L. Tuo, K. Yang, H.-K. Jeong, Y. Dai, G. He and W. Zhao, *J. Membr. Sci.*, 2016, **511**, 130–142.
66 J. Ma, Y. Ying, X. Guo, H. Huang, D. Liu and C. Zhong, *J. Mater. Chem. A*, 2016, **4**, 7281–7288.
67 R. Lin, L. Ge, H. Diao, V. Rudolph and Z. Zhu, *ACS Appl. Mater. Interfaces*, 2016, **8**, 32041–32049.
68 N. N. R. Ahmad, C. P. Leo, A. W. Mohammad and A. L. Ahmad, *Microporous Mesoporous Mater.*, 2017, **244**, 21–30.
69 G. Huang, A. P. Isfahani, A. Muchtar, K. Sakurai, B. B. Shrestha, D. Qin, D. Yamaguchi, E. Sivaniah and B. Ghalei, *J. Membr. Sci.*, 2018, **565**, 370–379.
70 A. Ilyas, N. Muhammad, M. A. Gilani, I. F. J. Vankelecom and A. L. Khan, *Sep. Purif. Technol.*, 2018, **205**, 176–183.
71 A. Jomekian, B. Bazooyar, R. M. Behbahani, T. Mohammadi and A. Kargari, *J. Membr. Sci.*, 2017, **524**, 652–662.
72 N. N. R. Ahmad, C. P. Leo, A. W. Mohammad and A. L. Ahmad, *Sep. Purif. Technol.*, 2018, **197**, 439–448.
73 H. Zhu, L. Wang, X. Jie, D. Liu and Y. Cao, *ACS Appl. Mater. Interfaces*, 2016, **8**, 22696–22704.
74 Z. Qiao, S. Zhao, J. Wang, S. Wang, Z. Wang and M. D. Guiver, *Angew. Chem., Int. Ed.*, 2016, **55**, 9321–9325.
75 A. A. Shamsabadi, F. Seidi, E. Salehi, M. Nozari, A. Rahimpour and M. Soroush, *J. Mater. Chem. A*, 2017, **5**, 4011–4025.
76 H. R. Amedi and M. Aghajani, *Microporous Mesoporous Mater.*, 2017, **247**, 124–135.
77 J. Zhang, Q. Xin, X. Li, M. Yun, R. Xu, S. Wang, Y. Li, L. Lin, X. Ding, H. Ye and Y. Zhang, *J. Membr. Sci.*, 2019, **570–571**, 343–354.
78 F. Li, Y. Li, T.-S. Chung and S. Kawi, *J. Membr. Sci.*, 2010, **356**, 14–21.
79 T. Zhou, L. Luo, S. Hu, S. Wang, R. Zhang, H. Wu, Z. Jiang, B. Wang and J. Yang, *J. Membr. Sci.*, 2015, **489**, 1–10.
80 Y. Ban, Y. Li, Y. Peng, H. Jin, W. Jiao, X. Liu and W. Yang, *Chem.–Eur. J.*, 2014, **20**, 11402–11409.
81 S. J. D. Smith, B. P. Ladewig, A. J. Hill, C. H. Lau and M. R. Hill, *Sci. Rep.*, 2015, **5**, 7823.
82 S. Wang, Y. Liu, M. Zhang, D. Shi, Y. Li, D. Peng, G. He, H. Wu, J. Chen and Z. Jiang, *J. Membr. Sci.*, 2016, **505**, 44–52.
83 D. Peng, Y. Liu, S. Wang, Z. Tian, Q. Xin, H. Wu, J. Chen and Z. Jiang, *RSC Adv.*, 2016, **6**, 65282–65290.
84 D. Peng, S. Wang, Z. Tian, X. Wu, Y. Wu, H. Wu, Q. Xin, J. Chen, X. Cao and Z. Jiang, *J. Membr. Sci.*, 2017, **522**, 351–362.
85 X. Zhang, T. Zhang, Y. Wang, J. Li, C. Liu, N. Li and J. Liao, *J. Membr. Sci.*, 2018, **560**, 38–46.
86 U. Cakal, L. Yilmaz and H. Kalipcilar, *J. Membr. Sci.*, 2012, **417–418**, 45–51.

Published on 04 October 2019. Downloaded by Yunnan University on 8/23/2025 5:29:10 PM.

87 S. Kanehashi, H. Gu, R. Shindo, S. Sato, T. Miyakoshi and K. Nagai, *J. Appl. Polym. Sci.*, 2013, **128**, 3814–3823.
88 R. Nasir, H. Mukhtar, Z. Man, M. S. Shaharun and M. Z. A. Bakar, *RSC Adv.*, 2015, **5**, 60814–60822.
89 L. Diestel, N. Wang, A. Schulz, F. Steinbach and J. Caro, *Ind. Eng. Chem. Res.*, 2015, **54**, 1103–1112.
90 D. Zhao, J. Ren, Y. Wang, Y. Qiu, H. Li, K. Hua, X. Li, J. Jia and M. Deng, *J. Membr. Sci.*, 2017, **521**, 104–113.
91 A. E. Amooghin, H. Sanaeepur, M. Omidkhahc and A. Kargari, *J. Mater. Chem. A*, 2018, **6**, 1751–1771.
92 H. Koolivand, A. Sharif, M. R. Kashani, M. Karimi, M. K. Salooki and M. A. Semsarzadeh, *J. Polym. Res.*, 2014, **21**, 599.
93 S. R. Venna, M. Lartey, T. Li, A. Spore, S. Kumar, H. B. Nulwala, D. R. Luebke, N. L. Rosi and E. Albenze, *J. Mater. Chem. A*, 2015, **3**, 5014–5022.
94 X. Gao, J. Zhang, K. Huang and J. Zhang, *ACS Appl. Mater. Interfaces*, 2018, **10**, 34640–34645.
95 G. Yu, X. Zou, L. Sun, B. Liu, Z. Wang, P. Zhang and G. Zhu, *Adv. Mater.*, 2019, **31**, 1806853.
96 M. Loloei, M. Omidkhah, A. Moghadassi and A. E. Amooghin, *Int. J. Greenhouse Gas Control*, 2015, **39**, 225–235.
97 R. Castro-Muñoz, V. Fíla, V. Martin-Gil and C. Muller, *Sep. Purif. Technol.*, 2019, **210**, 553–562.
98 A. Mahmoudi, M. Asghari and V. Zargar, *J. Ind. Eng. Chem.*, 2015, **23**, 238–242.
99 M. M. Khan, V. Filiz, G. Bengtson, S. Shishatskiy, M. Rahman and V. Abetz, *Nanoscale Res. Lett.*, 2012, **7**, 504.
100 M. M. Khan, V. Filiz, G. Bengtson, S. Shishatskiy, M. M. Rahman, J. Lillepaerg and V. Abetz, *J. Membr. Sci.*, 2013, **436**, 109–120.
101 D. K. Roh, S. J. Kim, W. S. Chi, J. K. Kim and J. H. Kim, *Chem. Commun.*, 2014, **50**, 5717–5720.
102 X. Li, Y. Cheng, H. Zhang, S. Wang, Z. Jiang, R. Guo and H. Wu, *ACS Appl. Mater. Interfaces*, 2015, **7**, 5528–5537.
103 K. Xie, Q. Fu, J. Kim, H. Lu, Y. He, Q. Zhao, J. Scofield, P. A. Webley and G. G. Qiao, *J. Membr. Sci.*, 2017, **535**, 350–356.
104 R. Xu, Z. Wang, M. Wang, Z. Qiao and J. Wang, *J. Membr. Sci.*, 2019, **573**, 455–464.
105 Q. Liu, N. Wang, J. Caro and A. Huang, *J. Am. Chem. Soc.*, 2013, **135**, 17679–17682.
106 A. Huang, Q. Liu, N. Wang and J. Caro, *J. Mater. Chem. A*, 2014, **2**, 8246–8251.
107 N. Wang, Y. Liu, Z. Qiao, L. Diestel, J. Zhou, A. Huang and J. Caro, *J. Mater. Chem. A*, 2015, **3**, 4722–4728.
108 W. Wu, Z. Li, Y. Chen and W. Li, *Environ. Sci. Technol.*, 2019, **53**, 3764–3772.
109 Z. Wang, D. Wang, S. Zhang, L. Hu and J. Jin, *Adv. Mater.*, 2016, **28**, 3399–3405.
110 L. Dong, M. Chen, X. Wu, D. Shi, W. Dong, H. Zhang and C. Zhang, *New J. Chem.*, 2016, **40**, 9148–9159.
111 W. Zhang, Y. Ying, J. Ma, X. Guo, H. Huang, D. Liu and C. Zhong, *J. Membr. Sci.*, 2017, **527**, 8–17.
112 L. Yu, F. Lin, W. Xiao, D. Luo and J. Xi, *J. Membr. Sci.*, 2018, **549**, 411–419.
113 L. Cao, F. Lv, Y. Liu, W. Wang, Y. Huo, X. Fu, R. Sun and Z. Lu, *Chem. Commun.*, 2015, **51**, 4364–4367.
114 Q. Xin, H. Wu, Z. Jiang, Y. Li, S. Wang, Q. Li, X. Li, X. Lu, X. Cao and J. Yang, *J. Membr. Sci.*, 2014, **467**, 23–35.
115 J. Kim, Q. Fu, K. Xie, J. M. P. Scofield, S. E. Kentish and G. G. Qiao, *J. Membr. Sci.*, 2016, **515**, 54–62.
116 H. Zhu, J. Yuan, J. Zhao, G. Liu and W. Jin, *Sep. Purif. Technol.*, 2019, **214**, 78–86.
117 X. Xu, C. Song, J. M. Andresen, B. G. Miller and A. W. Scaroni, *Energy Fuels*, 2002, **16**, 1463–1469.
118 R. Sanz, G. Calleja, A. Arencibia and E. S. Sanz-Pérez, *Appl. Surf. Sci.*, 2010, **256**, 5323–5328.
119 Z. Chen, S. Deng, H. Wei, B. Wang, J. Huang and G. Yu, *ACS Appl. Mater. Interfaces*, 2013, **5**, 6937–6945.
120 S. Xian, F. Xu, C. Ma, Y. Wu, Q. Xia, H. Wang and Z. Li, *Chem. Eng. J.*, 2015, **280**, 363–369.
121 Q. Wang, Y. Liu, J. Chen, Z. Du and J. Mi, *Environ. Sci. Technol.*, 2016, **50**, 7879–7888.
122 H. Wu, X. Li, Y. Li, S. Wang, R. Guo, Z. Jiang, C. Wu, Q. Xin and X. Lu, *J. Membr. Sci.*, 2014, **465**, 78–90.
123 Q. Xin, J. Ouyang, T. Liu, Z. Li, Z. Li, Y. Liu, S. Wang, H. Wu, Z. Jiang and X. Cao, *ACS Appl. Mater. Interfaces*, 2015, **7**, 1065–1077.
124 Y. K. Hwang, D.-Y. Hong, J.-S. Chang, S. H. Jhung, Y.-K. Seo, J. Kim, A. Vimont, M. Daturi, C. Serre and G. Férey, *Angew. Chem., Int. Ed.*, 2008, **47**, 4144–4148.
125 M. Wickenheisser, F. Jeremias, S. K. Henninger and C. Janiak, *Inorg. Chim. Acta*, 2013, **407**, 145–152.
126 X. Guo, H. Huang, D. Liu and C. Zhong, *Chem. Eng. Sci.*, 2018, **189**, 277–285.
127 Y. Gao, Z. Qiao, S. Zhao, Z. Wang and J. Wang, *J. Mater. Chem. A*, 2018, **6**, 3151–3161.
128 Y. Cheng, L. Zhai, Y. Ying, Y. Wang, G. Liu, J. Dong, D. Z. L. Ng, S. A. Khana and D. Zhao, *J. Mater. Chem. A*, 2019, **7**, 4549–4560.
129 H. S. M. Suhaimi, M. N. I. M. Khir, C. P. Leo and A. L. Ahmad, *J. Polym. Res.*, 2014, **21**, 428.
130 Y. Liu, D. Peng, G. He, S. Wang, Y. Li, H. Wu and Z. Jiang, *ACS Appl. Mater. Interfaces*, 2014, **6**, 13051–13060.
131 H. Zhang, R. Guo, J. Hou, Z. Wei and X. Li, *ACS Appl. Mater. Interfaces*, 2016, **8**, 29044–29051.
132 B. Prasad and B. Mandal, *ACS Appl. Mater. Interfaces*, 2018, **10**, 27810–27820.
133 Q. Xin, H. Liu, Y. Zhang, H. Ye, S. Wang, L. Lin, X. Ding, B. Cheng, Y. Zhang, H. Wu and Z. Jiang, *J. Membr. Sci.*, 2017, **525**, 330–341.
134 Y. Wang, X. Zhang, J. Li, C. Liu, Y. Gao, N. Li and Z. Xie, *J. Membr. Sci.*, 2019, **573**, 602–611.
135 H. Wang, S. He, X. Qin, C. Li and T. Li, *J. Am. Chem. Soc.*, 2018, **140**, 17203–17210.
136 Q. Qian, A. X. Wu, W. S. Chi, P. A. Asinger, S. Lin, A. Hypsher and Z. P. Smith, *ACS Appl. Mater. Interfaces*, 2019, **11**, 31257–31269.
137 X. Cao, Z. Wang, Z. Qiao, S. Zhao and J. Wang, *ACS Appl. Mater. Interfaces*, 2019, **11**, 5306–5315.
138 Y. Katayama, K. C. Bentz and S. M. Cohen, *ACS Appl. Mater. Interfaces*, 2019, **11**, 13029–13037.

 This journal is © The Royal Society of Chemistry 2019

Published on 04 October 2019. Downloaded by Yunnan University on 8/23/2025 5:29:10 PM.

139 C. H. Hendon, A. J. Rieth, M. D. Korzyński and M. Dincă, *ACS Cent. Sci.*, 2017, **3**, 554–563.
140 P. Silva, S. M. F. Vilela, J. P. C. Tomé and F. A. A. Paz, *Chem. Soc. Rev.*, 2015, **44**, 6774–6803.
141 J.-R. Li, J. Scculley and H.-C. Zhou, *Chem. Rev.*, 2012, **112**, 869–932.
142 M. S. Lohse and T. Bein, *Adv. Funct. Mater.*, 2018, **28**, 1705553.
143 I. Erucar and S. Keskin, *J. Membr. Sci.*, 2012, **407–408**, 221–230.
144 B. Zornoza, B. Seoane, J. M. Zamaro, C. Téllez and J. Coronas, *ChemPhysChem*, 2011, **12**, 2781–2785.
145 H. B. T. Jeazet, S. Sorribas, J. M. Román-Marín, B. Zornoza, C. Téllez, J. Coronas and C. Janiak, *Eur. J. Inorg. Chem.*, 2016, 4363–4367.
146 C. Casado-Coterillo, A. Fernández-Barquín, B. Zornoza, C. Téllez, J. Coronas and Á. Irabien, *RSC Adv.*, 2015, **5**, 102350–102361.
147 L. Hao, P. Li, T. Yang and T.-S. Chung, *J. Membr. Sci.*, 2013, **436**, 221–231.
148 İ. Ayas, L. Yilmaz and H. Kalipcilar, *Ind. Eng. Chem. Res.*, 2018, **57**, 16041–16050.
149 W. Li, S. A. S. C. Samarasinghe and T.-H. Bae, *J. Ind. Eng. Chem.*, 2018, **67**, 156–163.
150 R. Castro-Muñoz and V. Fíla, *Chem. Eng. Technol.*, 2019, **42**, 744–752.
151 M. Barooah and B. Mandal, *J. Membr. Sci.*, 2019, **572**, 198–209.
152 H. Mahdavi and F. Moradi-Garakani, *Chem. Eng. Res. Des.*, 2017, **125**, 156–165.
153 M. Sarfraz and M. Ba-Shammakh, *J. Ind. Eng. Chem.*, 2016, **36**, 154–162.
154 M. Sarfraz and M. Ba-Shammakh, *J. Membr. Sci.*, 2016, **514**, 35–43.
155 M. Sarfraz and M. Ba-Shammakh, *Polym. Bull.*, 2018, **75**, 5039–5059.
156 M. Sarfraz and M. Ba-Shammakh, *Arabian J. Sci. Eng.*, 2016, **41**, 2573–2582.
157 M. Sarfraz and M. Ba-Shammakh, *Braz. J. Chem. Eng.*, 2018, **35**, 217–228.
158 S. A. S. C. Samarasinghe, C. Y. Chuah, Y. Yang and T.-H. Bae, *J. Membr. Sci.*, 2018, **557**, 30–37.
159 A. Galve, D. Sieffert, C. Staudt, M. Ferrando, C. Güell, C. Téllez and J. Coronas, *J. Membr. Sci.*, 2013, **431**, 163–170.
160 M. Valero, B. Zornoza, C. Téllez and J. Coronas, *Microporous Mesoporous Mater.*, 2014, **192**, 23–28.
161 S. Sorribas, B. Zornoza, C. Téllez and J. Coronas, *J. Membr. Sci.*, 2014, **452**, 184–192.
162 R. Lin, L. Ge, S. Liu, V. Rudolph and Z. Zhu, *ACS Appl. Mater. Interfaces*, 2015, **7**, 14750–14757.
163 Z. Song, F. Qiu, E. W. Zaia, Z. Wang, M. Kunz, J. Guo, M. Brady, B. Mi and J. J. Urban, *Nano Lett.*, 2017, **17**, 6752–6758.
164 J. Sánchez-Laínez, A. Veiga, B. Zornoza, S. R. G. Balestra, S. Hamad, A. R. Ruiz-Salvador, S. Calero, C. Télleza and J. Coronas, *J. Mater. Chem. A*, 2017, **5**, 25601–25608.
165 J. Sánchez-Laínez, B. Zornoza, A. F. Orsi, M. M. Łozińska, D. M. Dawson, S. E. Ashbrook, S. M. Francis, P. A. Wright, V. Benoit, P. L. Llewellyn, C. Téllez and J. Coronas, *Chem.–Eur. J.*, 2018, **24**, 11211–11219.
166 Y. Cheng, Y. Ying, L. Zhai, G. Liu, J. Dong, Y. Wang, M. P. Christopher, S. Long, Y. Wang and D. Zhao, *J. Membr. Sci.*, 2019, **573**, 97–106.
167 L. Dong, M. Chen, J. Li, D. Shi, W. Dong, X. Li and Y. Bai, *J. Membr. Sci.*, 2016, **520**, 801–811.
168 H. Lee, S. C. Park, J. S. Roh, G. H. Moon, J. E. Shin, Y. S. Kang and H. B. Park, *J. Mater. Chem. A*, 2017, **5**, 22500–22505.
169 S. Castarlenas, C. Téllez and J. Coronas, *J. Membr. Sci.*, 2017, **526**, 205–211.
170 D. Huang, Q. Xin, Y. Ni, Y. Shuai, S. Wang, Y. Li, H. Ye, L. Lin, X. Ding and Y. Zhang, *RSC Adv.*, 2018, **8**, 6099–6109.
171 M. Jia, Y. Feng, J. Qiu, X.-F. Zhang and J. Yao, *Sep. Purif. Technol.*, 2019, **213**, 63–69.
172 K. Yang, Y. Dai, W. Zheng, X. Ruan, H. Li and G. He, *Sep. Purif. Technol.*, 2019, **214**, 87–94.
173 N. Zhang, H. Wu, F. Li, S. Dong, L. Yang, Y. Ren, Y. Wu, X. Wu, Z. Jiang and X. Cao, *J. Membr. Sci.*, 2018, **567**, 272–280.
174 F. de Clippel, A. L. Khan, A. Cano-Odena, M. Dusselier, K. Vanherck, L. Peng, S. Oswald, L. Giebeler, S. Corthals, B. Kenens, J. F. M. Denayer, P. A. Jacobs, I. F. J. Vankelecom and B. F. Sels, *J. Mater. Chem. A*, 2013, **1**, 945–953.
175 M. W. Anjum, F. de Clippel, J. Didden, A. L. Khan, S. Couck, G. V. Baron, J. F. M. Denayer, B. F. Sels and I. F. J. Vankelecom, *J. Membr. Sci.*, 2015, **495**, 121–129.
176 X. Li, L. Ma, H. Zhang, S. Wang, Z. Jiang, R. Guo, H. Wu, X. Cao, J. Yang and B. Wang, *J. Membr. Sci.*, 2015, **479**, 1–10.
177 G. Dong, X. Zhang, Y. Zhang and T. Tsuru, *ACS Sustainable Chem. Eng.*, 2018, **6**, 8515–8524.
178 J. E. Shin, S. K. Lee, Y. H. Cho and H. B. Park, *J. Membr. Sci.*, 2019, **572**, 300–308.
179 J. Hou, X. Li, R. Guo, Y. Qin and J. Zhang, *Polym. Compos.*, 2018, **39**, 4486–4495.
180 C. A. Dunn, Z. Shi, R. Zhou, D. L. Gin and R. D. Noble, *Ind. Eng. Chem. Res.*, 2019, **58**, 4704–4708.
181 Y. Lan, X. Han, M. Tong, H. Huang, Q. Yang, D. Liu, X. Zhao and C. Zhong, *Nat. Commun.*, 2018, **9**, 5274.
182 C. Zhang, Y. Lan, X. Guo, Q. Yang and C. Zhong, *AIChE J.*, 2018, **64**, 1389–1398.
183 P. G. Boyd, Y. Lee and B. Smit, *Nat. Rev. Mater.*, 2017, **2**, 17037.
184 Y. Lan, T. Yan, M. Tong and C. Zhong, *J. Mater. Chem. A*, 2019, **7**, 12556–12564.
185 T. Rodenas, M. van Dalen, E. García-Pérez, P. Serra-Crespo, B. Zornoza, F. Kapteijn and J. Gascon, *Adv. Funct. Mater.*, 2014, **24**, 249–256.
186 T. Rodenas, I. Luz, G. Prieto, B. Seoane, H. Miro, A. Corma, F. Kapteijn, F. X. Llabrés i Xamena and J. Gascon, *Nat. Mater.*, 2015, **14**, 48–55.